Performance Enhancement of Active Power Filter using Robust Control Strategies

Soumya Ranjan Mohapatra

Department of Electrical Engineering
National Institute of Technology Rourkela
Rourkela-769008, India

Performance Enhancement of Active Power Filter using Robust Control Strategies

A thesis submitted in partial fulfilment of the requirements for the award of the award of degree

Master of Technology by Research

in

Electrical Engineering

by

Soumya Ranjan Mohapatra

Roll No: 612EE101

Under the Guidance of

Prof. Pravat Kumar Ray

Department of Electrical Engineering

National Institute of Technology Rourkela

Rourkela-769008, India

2012-2014

Department of Electrical Engineering
National Institute of Technology, Rourkela

CERTIFICATE

This to certify that the thesis titled "**Performance Enhancement of Active Power Filter using Robust Control Strategies**", by ***Mr. Soumya Ranjan Mohapatra*** submitted to the National Institute of Technology Rourkela for the award of Master of Technology by Research in Electrical Engineering is a record of bonafide research work carried out by him in the Department of Electrical Engineering, under my supervision. We believe that this thesis fulfils part of the requirements for the award of the degree of Master of Technology by Research. The results embodied in this thesis have not been submitted for the award of any degree elsewhere.

Place: Rourkela **Prof. Pravat Kumar Ray**

Date:

Dedicated

To

Lord Jagannath

…Soumya Ranjan Mohapatra

Acknowledgement

First and foremost, I am deeply grateful to my supervisor **Prof. Pravat Kumar Ray** for his impetus, excellence guidance. I would like to express my gratitude to the members of Masters Scrutiny Committee, **Prof.B.D.Subudhi**, **Prof.S.Ganguly** and **Prof.S.K.Behera** for their advice. I am also very much obliged to **Prof. Anup Ku Panda** Head of the Department of Electrical Engineering, N.I.T Rourkela for providing all the possible facilities towards this research work. Also thank to other faculty members in the department.

I am also thankful to laboratory staff of Control and Research lab, Power Electronics lab and office staff of our department for their excellent service and help.

I am very much grateful to my senior research scholars Sushree Diptimayee Swain, Pradeep Kumar Sahoo, Jitendra kumar Jain and my research colleagues Debashis Mohapatra, Soumya ranjan Mahapatro and all research members of Control and Robotics Lab and power electronics lab of NIT Rourkela for their cooperation and help.

I am appreciative to Mr and Mrs Sarat Chaine, Srihari Nayak, Maheswar Behera, Swarnabala Upadhyaya, Jyotirmayee Dalei and Soumya Mishra for their inspiration, mental support and constant encouragement throughout my M. Tech (R) journey.

I would also like to acknowledge the Ministry of Human Resource and Development, India (MHRD) for the grant of scholarship for the last two years to pursue the research.

I also express my deep gratitude to my parents Chunibala Mohapatra and Niranjan Mohapatra and my sister Sonya Mohapatra for their love, support and encouragement.

Soumya Ranjan Mohapatra

Abstract

The prime focus of this thesis is to report control strategies to improve the performance of single phase shunt Active Power Filter (APF). Basically, Sliding Mode (SM) control strategy and Feedback Linearization based control strategy have been applied considering their ease of implementation and robustness under external disturbances. An low cost analog SM controller is presented to reduce the steady state current error. In this method a band pass filter is used for calculating the reference source current which makes source current Total Harmonic Distortion (THD) independent of source voltage THD. Multisim based simulation method and results are presented to report the method of low cost analog implementation. To overcome the drawbacks caused by varying switching frequency, a fixed switching frequency SM controller is presented, in which Artificial Neural Network (ANN) is used to generate the reference source current. In this control strategy, a proper combination of fixed frequency sliding mode current control, ANN based fundamental source current extraction circuit and unipolar PWM increases the dynamic response of APF system and makes it adaptive under variable load and source conditions.

As feedback linearization based controller improves the performance of the power electronic systems by analysing stability of the complete system, a straight forward Partial Feedback Linearization (PFL) based control strategy is presented to reduce the source current THD of single phase shunt APF. The nonlinear system dynamics of the APF has been partially feedback linearized using its average dynamic model. New control input to the linearized system is obtained considering the stability of the complete APF system. After that, control input to APF is derived by nonlinear transformation. Stability of the internal dynamics of the system is analysed considering zero dynamics of the system. A prototype of the APF system is built and the proposed controller is implemented using dSPACE 1104. Both experimental and simulation results of the PFL based control strategy are compared with exact feedback linearization of APF via SM control for validation of performance improvement. Finally the application of PFL based control strategy is extended to three phase APF by considering it as Multiple Input Multiple Output (MIMO) system and MATLAB/Simulink based simulation results are presented to validate the theory.

Contents

	Abstract	v
	Contents	vi
	List of Figures	viii
	List of Tables	xi
	List of Abbreviations	xii
Chapter-1	**Introduction**	
1.1	Background	1
	1.1.1 Active Power Filter	2
	1.1.2 Shunt Active Power Filter	2
	1.1.3 Design of Active Power Filter Circuit	5
1.2	Literature Review on Control Strategies Applied to Shunt Active Power Filter and other Power Electronic Circuits	7
	1.2.1 Control of DC capacitor voltage along with generation of reference source current	7
	1.2.2 Switching scheme	8
	1.2.3 Current control of APF	10
	1.2.3.1 Sliding Mode Control	11
	1.2.3.2 Feedback Linearization based control	12
1.3	Research Motivation	14
1.4	Thesis Objectives	14
1.5	Thesis Organization	15
Chapter-2	**Design of an Analog Sliding Mode Controller for Single Phase Shunt Active Power Filter**	
2.1	Introduction	17
2.2	Chapter Objectives	17
2.3	Dynamic Model of Single Phase Shunt Active Power Filter	18
2.4	Development of Control Algorithm	19
	2.4.1 Sliding Mode Current Control of APF	19
	2.4.2 Reference Source Current Calculation	21
2.5	MATLAB/Simulink based Simulation Results	21
2.6	Multisim based Simulation Results	24
2.7	Chapter Summary	27
Chapter-3	**A Constant Switching Frequency adaptive Sliding Mode Current Control Design for Shunt Active Power Filter System**	

3.1	Introduction	28
3.2	Chapter Objectives	29
3.3	Development of Control Algorithm	29
	3.3.1 Fixed Switching Frequency Sliding Mode Current Controller	30
	3.3.2 Modified Artificial Neural Network Based Control Strategy	33
3.4	Results and Discussions	36
3.5	Chapter Summary	43
Chapter-4	**A Partial Feedback Linearization based Approach to Single Phase Shunt Active Power Filter Design**	
4.1	Introduction	44
4.2	Chapter Objectives	45
4.3	Averaged Dynamic Model of Single Phase Shunt Active Power Filter	45
4.4	Feedback Linearization based Controller Design for Shunt APF	47
	4.4.1 Partial Feedback Linearization	47
	4.4.2 Exact Feedback Linearization	50
4.5	Results and Discussions	53
	4.5.1 Simulation Results	53
	4.5.2 Experimental Results	56
4.6	Chapter Summary	59
Chapter-5	**A Partial Feedback Linearization based Control Design and Simulation for Three Phase Shunt Active Power Filter**	
5.1	Introduction	60
5.2	Chapter Objectives	60
5.3	Averaged Dynamic Model of Three Phase Shunt APF	61
5.4	Partial Feedback Linearization based Controller Design for Three Phase APF	64
5.5	Results and Discussions	67
5.6	Chapter Summary	69
Chapter-6	**Conclusions and Suggestions for Future Work**	
7.1	Conclusions	70
7.2	Contributions of the Thesis	71
7.3	Suggestions for the Future Work	71
	References	72

List of Figures

Sl No	Description	Page No
1.1	Block diagram of shunt active power filter	2
1.2	Block diagram of VSI based shunt active power filter	3
1.3	Block diagram of CSI based shunt active power filter	3
1.4	Typical structure single phase of shunt active power filter	4
1.5	Typical structure three phase of shunt active power filter	5
1.6	Switching scheme. (a) Source current, (b) Unipolar Modulation, (c) Bipolar Modulation	9
1.7	Sliding conditions (E) stable system (F) unstable system	12
2.1	Analog sliding mode controller for shunt APF	20
2.2	Source voltage (bottom). Load current (top). Analog SM controller	22
2.3	Nominal voltage source. Source voltage (bottom). Source current (top). Analog SM controller	22
2.4	Distorted voltage source. Source current (top). Source voltage (bottom). Analog SM controller	22
2.5	Filter Capacitor voltage (top). Inductor current (bottom). Analog SM controller	22
2.6	Source current (I_S) and reference Source current (I_{Sref}) with sliding surface $S = e_1 = I_S - I_{S\ ref}$	23
2.7	Source current (I_S) and reference Source current (I_{Sref}) with sliding surface $S = e_1 + \lambda e_2$	23
2.8	Filter capacitor voltage (bottom). Source current (top). Dynamic response for step load change	23
2.9	The schematic of analog SM controller for shunt APF	25
2.10	Multisim based simulation results. Nominal source. Source voltage (bottom). Load current (top). Analog SM controller	26
2.11	Multisim based simulation results. Nominal source. Source voltage (bottom). Source current (top). Analog SM controller	26
2.12	Multisim based simulation results. Distorted source. Source voltage (bottom). Source current (top). Analog SM controller	26
2.13	Multisim based simulation results. Nominal source. Filter capacitor voltage (bottom). Inductor current (top). Analog SM controller	26
3.1	Existence condition	30
3.2	Fixed frequency adaptive sliding mode controller	33
3.3	Modified ANN based extraction circuit	34
3.4	Source voltage (top). Load current (bottom). Nominal source. Fixed frequency adaptive SM controller	39

3.5	Source voltage (top). Source current (bottom). Nominal source. Fixed frequency adaptive SM controller	39
3.6	Source voltage (top). Load current (bottom). Distorted source. Fixed frequency adaptive SM controller	40
3.7	Source voltage (top). Source current (bottom). Distorted source. Fixed frequency adaptive SM controller	40
3.8	Load real power (top). Source voltage (middle). Load current (bottom). High to low nonlinear load. Fixed frequency adaptive SM controller	40
3.9	Load real power (top). Source voltage (middle), Load current (bottom). Low to high nonlinear load. Fixed frequency adaptive SM controller	40
3.10	Source voltage frequency (top). Source voltage (middle). Source current (bottom). High to low frequency variation. Fixed frequency adaptive SM controller	40
3.11	Source voltage frequency (top). Source voltage (middle). Source current (bottom). Low to high frequency variation. Fixed frequency adaptive SM controller	40
3.12	Compensating current (top). Error signal (bottom). Nominal source. Fixed frequency adaptive SM controller	41
3.13	Response of APF capacitor voltage. Nominal source. Fixed frequency adaptive SM controller	41
3.14	Power consumed by non-linear load. Real power (top). Reactive power (bottom).). Nominal source. Fixed frequency adaptive SM controller	41
3.15	Power delivered by non-linear load. Real power (top). Reactive power (bottom).). Nominal source. Fixed frequency adaptive SM controller	41
4.1	Single phase shunt active power	46
4.2	Equivalent circuit of active power filter. (a) $0 \le t \le uT$ (b) $uT \le t \le T$	46
4.3	Proposed PFL based controller	48
4.4	Phase plot of zero dynamics of APF in PFL based controller	50
4.5	Controller implemented in [3]	52
4.6	Source voltage (bottom). Load current (top). PFL based controller	54
4.7	Source voltage (bottom). Source current (top). PFL based controller	54
4.8	Source voltage (bottom). Source current (top). Controller reported in [3]	54
4.9	Response for load change. Load current (bottom). Source current (top). PFL based controller	54
4.10	Response for load change. Load current (bottom). Source current (top). Controller reported in [3]	55
4.11	Tracking of sliding surface trajectory, ‘S’ as per (4.28) top, ‘S’ as per (4.29) bottom. Controller reported in [3]	55
4.12	Filter capacitor voltage. PFL based controller	55
4.13	Inductor current. PFL based controller	55
4.14	Variation of THD with parameter inductance. PFL based controller	55
4.15	Block diagram of Hardware structure	57

4.16	The prototype of the experimental setup	57
4.17	Source voltage (bottom). Load current (top). Experimental results	58
4.18	Source voltage (bottom). Source current (top). Experimental results. PFL based controller	58
4.19	Filter capacitor voltage. Experimental results. PFL based controller	58
4.20	Source voltage (bottom). Source current (top). Experimental results. Controller reported in [3]	58
5.1	Three phase shunt active power filter	61
5.2	Equivalent circuit for phase 1 of three phase active power filter.	62
5.3	PFL based controller for three phase APF	65
5.4	Source voltage (bottom). Load current (top). PFL based controller for three phase APF	68
5.5	Source voltage (bottom). Source current (top). PFL based controller for three phase APF	68
5.6	Response for load change. Load current (bottom). Source current (top). PFL based controller for three phase APF	68
5.7	Filter capacitor voltage (bottom). Compensating current (top). PFL based controller for three phase APF	68

List of Tables

Sl No	Description	Page No
2.1	Switching scheme used in analog SM controller	19
2.2	System parameters used for MATLAB/Simulation in analog SM controller	22
3.1	Switching states and control input	29
3.2	System parameters used for MATLAB/Simulation in fixed frequency adaptive SM controller	39
3.3	Comparative performance analysis of fixed frequency adaptive SM controller	42
4.1	Switching scheme used in [1]	52
4.2	Switching scheme used in [3]	52
4.3	Concept behind the use of XOR gate	53
4.4	System parameters used for Simulation for comparative analysis of both PFL and EFL based controller	54
5.1	System parameters used for Simulation in PFL based controller for three phase APF	67

List of Abbreviations

Abbreviations	Description
APF	Active Power Filter
SM	Sliding Mode
PFL	Partial Feedback Linearization
EFL	Exact Feedback Linearization
PWM	Pulse Width Modulation
PI	Proportional- Integral
PD	Proportional- Derivative
ANN	Artificial Neural Network
PLL	Phase Locked Lop
THD	Total Harmonic Distortion
RC	Resister Capacitor
DC	Direct Current
AC	Alternating Current
SISO	Single Input Single Output
MIMO	Multiple Input Multiple Output
IGBT	Insulated Gate Bipolar Transistor
VSI	Voltage Source Inverter
CSI	Current Source Inverter
MOSFET	Metal Oxide Semiconductor Field Effect Transistor
HM	Hysteresis Modulation

CHAPTER 1

INTRODUCTION

1.1. Background

Now a days people are extremely dependent on use of nonlinear loads. All the power electronic devices can be considered as nonlinear loads. Controlled/uncontrolled rectifiers, inverters, uninterruptable power supplies, switched mode power supplies, televisions, refrigerators, printers, fax machines, fluorescent lamps, adjustable speed drives, air conditioners are some examples of nonlinear loads. The use of nonlinear loads causes harmonic distortion. Harmonics of a sinusoidal waveform are sinusoidal waveforms having frequency integral multiple of frequency of the original sinusoidal waveform. In electrical engineering, voltage and current waveforms plays an important role in the reliability of electrical devices. In India the fundamental frequency of voltage waveform is 50Hz, while in some of the foreign countries fundamental frequency of voltage signal is 60 Hz. When fundamental frequency is 50 Hz, the 2^{nd} harmonic is 100 Hz, 3^{rd} harmonic is 150 Hz and so on. The presence of these harmonics in voltage or current waveforms is known as harmonic distortion. A major term related to harmonics is Total Harmonic distortion (THD). THD of a signal is calculated as the square root of sum of squares of all the harmonics present in that signal. There are several problems caused due to voltage and current harmonic distortion, such as: overheating of motors, transformers and capacitors, increase in conduction losses and eddy current losses, premature damage of electrical equipment, important data loss from computers used in offices, meter readings with higher percentage of error, etc. Therefore mitigation of harmonics from voltage and current wave forms has become a major concern of power and control researchers. Including harmonic distortion, there are also several other factors, such as voltage sag, voltage swell, voltage flicker, etc., which hampers the power quality.

Passive filters have been used to improve the power quality by compensating voltage and current harmonics, but these are no longer used due to high cost, large size and resonance effect.

Also there is no possibility of using same passive filter for different loads. These problems can be overcome by use of active power filter (APF).

1.1.1. Active Power Filter

APF not only mitigates harmonics from voltage and current waveforms but also improves power factor, reduces neutral current of three phase AC supply, compensates the reactive power, adapts itself to different load and source conditions and reduces the impact of voltage sag, swell and flicker. All these simultaneous work can be possible only due to closed loop switching control application of APF.

APF is a power electric equipment connected either in series or in parallel or combination of both in between source and load. Depending on its connection it is classified into three categories, namely: 1) series APF; 2) shunt APF; 3) universal APF or unified power line conditioner. Series APF is used to compensate voltage harmonics, while shunt APF is used to compensate current harmonics. Universal APF is used to compensate voltage harmonics as well as current harmonics. Sometimes a combination of both APF and passive filter is used for better result. This type of filter is known as hybrid active power filter. Due to requirement of current harmonic compensation in most of the industrial applications, performance improvement of shunt active power filter has become the choice of many researchers.

1.1.2. Shunt Active Power Filter

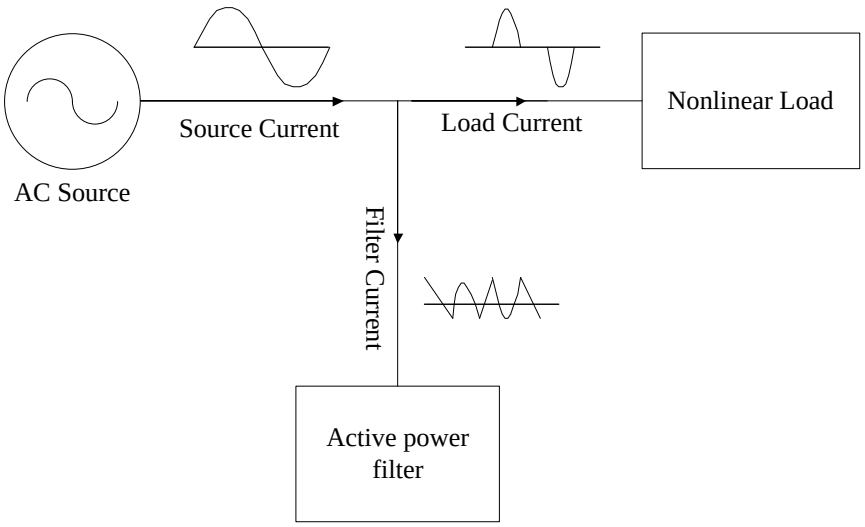

Fig.1.1 Block diagram of shunt active power filter

Shunt APF is connected in parallel at the Point of Common Coupling (PCC) in between source and nonlinear load. Main focus of shunt APF design is to compensate current harmonics caused by nonlinear load by supplying equal amount of harmonics at PCC but with opposite polarity. Block diagram of shunt APF is shown in Fig.1.1. APF is an inverter with some controllable switches. A voltage source inverter (VSI) or a current source inverter (CSI) can be used as an APF.

In CSI based APF, a CSI is connected at PCC through second order low pass filter made up of L_F and C_F as shown in Fig. 1.3. Current source of the inverter is replaced by a high DC side inductor [36]. In CSI all the semiconductor switches must support unipolar current and bipolar voltage. Earlier researchers were using Gate Turn-Off (GTO) thyristor with reverse blocking capabilities. But now a days to enhance research on CSI, Insulated Gate Bipolar Transistor (IGBT) with a series diode are available in market.

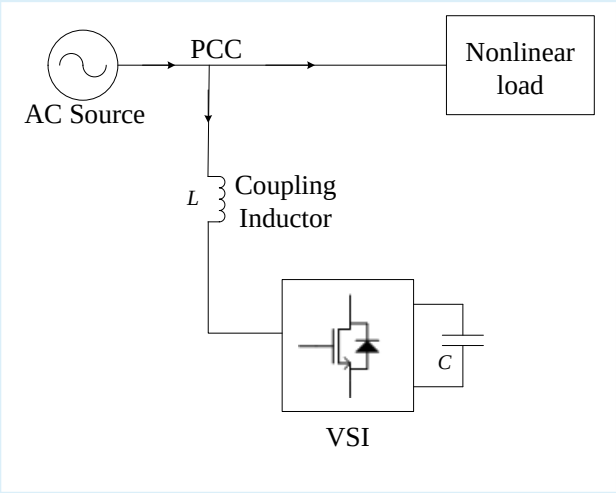

Fig. 1.2 Block diagram of VSI based shunt active power filter

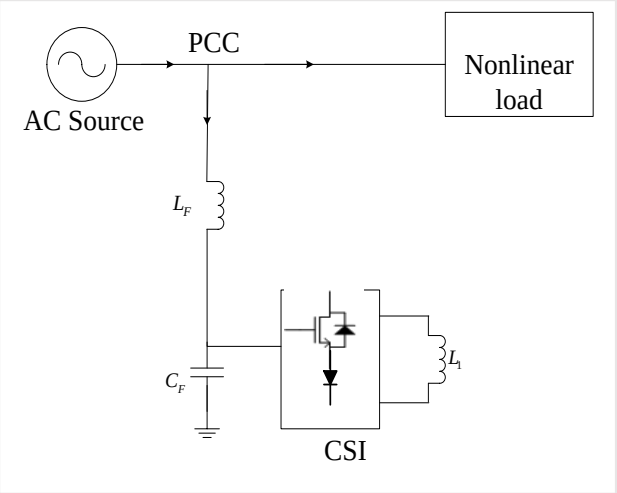

Fig. 1.3 Block diagram of CSI based shunt active power filter

In VSI, the AC side of the inverter is connected at PCC through a coupling inductor. In the DC side of VSI, DC source of inverter can be replaced by a large capacitor as there is no resistive element used in the AC side of the inverter. As all the circuit elements are not ideal, some steps should be taken to overcome the internal resistance of the circuit elements while using VSI as APF. This is discussed in latter parts of the thesis. All switches must support bipolar current and unipolar voltage. So semiconductor switches with anti-parallel diode are generally used. Block diagram of VSI based shunt APF is shown in Fig. 1.2.

Coming into the benefits and drawbacks of both VSI and CSI based shunt APF, CSI fed APF is very efficient in low power conditions. But it is comparatively heavier than the VSI fed APF. Also CSI fed APF has high DC link losses due to use of large inductor in the DC side of CSI. The major drawback associated with VSI fed APF is that there is switching ripple in the source current after compensation. There is no such significant difference in harmonic compensation characteristics of both VSI and CSI fed APF. But considering ease of implementation of VSI fed APF, its performance development is considered in this thesis.

Depending on the AC source and load, APF configuration is also changed. For a single phase source, single phase shunt APF is used and for a three phase source a three phase APF is used. Generally for household and office applications such as: computers, fax machines, printers, etc, single phase supply is used. So single phase shunt APFs are widely used to eliminate current harmonics in this field [1-5]. A single phase shunt APF is shown in Fig. 1.4. As shown in Fig.1.4, the variable I_S, I_O and I_L are used to present the source current, output current and inductor current respectively. V_S and V_C presents the source voltage and capacitor voltage respectively. Resistance 'R'is used to demonstrate all the internal resistances of the circuit elements. In [2] and [4] this resistance R is considered in the analysis of control strategy of APF, whereas in [29] this resistance is neglected. A single phase diode bridge rectifier with RC load used as a nonlinear load as shown in Fig. 1.4.

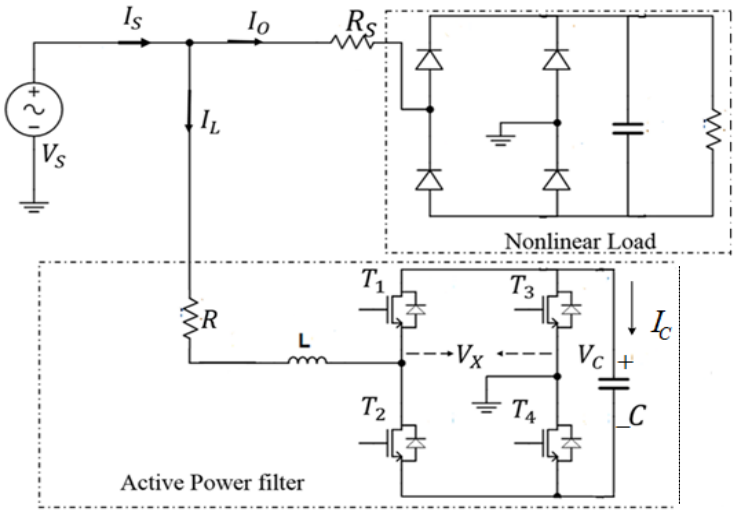

Fig. 1.4 Typical structure single phase of shunt active power filter

Similarly for industry applications to eliminate current harmonics three phase shunt APF is required. A typical structure of three phase shunt APF is shown in Fig 1.5 as per [38]. Three phase bridge rectifier with *RCL* load used as nonlinear load. A three phase VSI with large DC capacitor, coupled to the AC mains through coupling inductors acts as a three phase APF. Circuit elements are named as in Fig. 1.4 and Fig. 1.5.

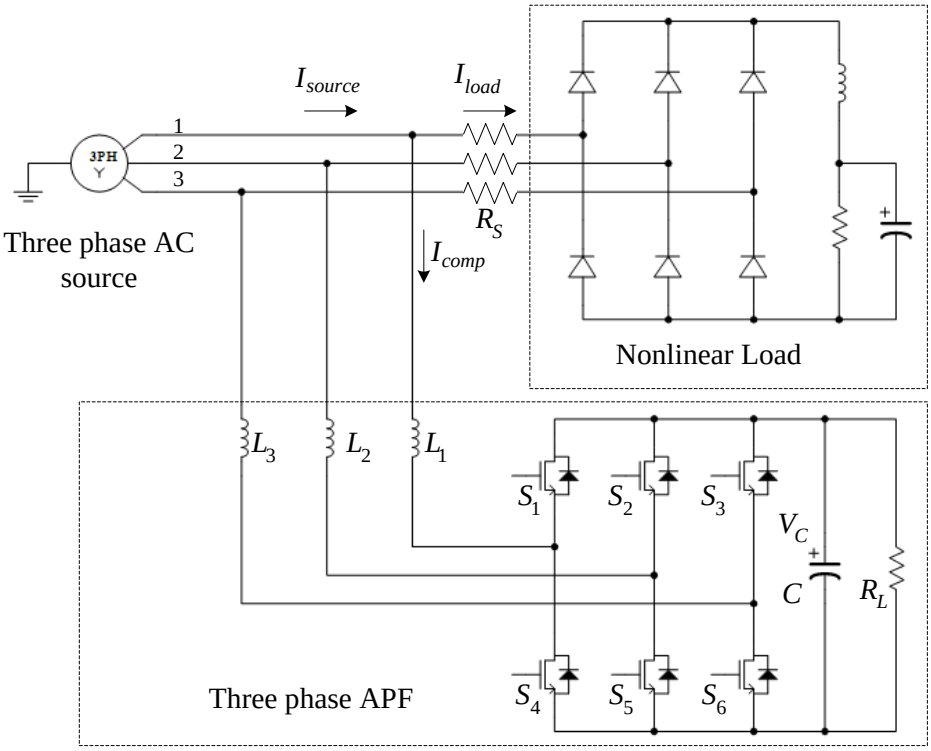

Fig. 1.5 Typical structure three phase of shunt active power filter

1.1.3. Design of the circuit of APF

The design of the APF circuit mainly includes the following factors:

- Choosing controlled switches
- Selecting the Value of DC link filter capacitor
- Choosing the value(s) of coupling inductor (s)
- Taking a reference DC capacitor voltage.

Metal Oxide Semiconductor Field Effect Transistor (MOSFET) or IGBT switches with a antiparallel diode across it can be used as switches in shunt APF. The voltage and current rating

of the switches must be higher than peak DC link Filter capacitor voltage and peak coupling inductor current respectively. The peak of coupling inductor current can be determined easily by knowing nonlinear load model [1]. Coupling inductor current is for a single phase shunt APF

$$I_L = I_{Source} - I_{load} \tag{1.1}$$

where I_L is the coupling inductor current. As per literature [1], I_{Source} can be calculated as follows:

$$I_{Source} = \frac{\sqrt{2}P_{load}}{V_{rms}}\sin(\omega t) \tag{1.2}$$

P_{load} is real power consumed by nonlinear load and ωt is the instantaneous phase of the source voltage. The current rating of the APF semiconductor switches is taken higher than the peak of the inductor current considering inductor current ripples and other factors. The smaller is the inductor, the higher is the ripple and vice versa. But inductor with high inductance does not allow the compensating current to flow within it. Considering these two aspects, the value of inductor is chosen suitably.

To shape the line current at any instant of time, the reference DC capacitor voltage must be higher than the peak of the source voltage for a single phase shunt APF [1]. Similarly for a three phase shunt APF the reference DC capacitor voltage must be greater than two times to that of source voltage as per [15]. As this DC reference capacitor voltage does not have any impact on THD of source current, it can be taken randomly satisfying the above said conditions. But to make APF work properly under sudden load change, one has to consider another point for choosing the reference DC capacitor voltage. In this case for a single phase shunt APF the DC reference capacitor voltage must be greater than sum of peak value of source voltage and real power difference in step load changes. Similar steps should be taken for three phase APF. The DC capacitor is used for two important purposes, such as: 1) to maintain DC voltage level higher than the peak of source voltage. 2) to supply the real power difference during sudden load changes. Considering these two aspects a large value of capacitor is selected as follows [39]:

$$C = \frac{\triangle E_{MAX}}{V_{DC} - V_{DC\ MIN}} \tag{1.3}$$

$\triangle E_{MAX}$ is max real power difference during step load changes, that capacitor has to supply during

transient condition. V_{DC} is chosen as the reference capacitor voltage and $V_{DC\ MIN}$ is the minimum reference capacitor voltage, which can be taken.

Considering capacitor voltage ripple, the voltage rating of the semiconductor controllable switches must be higher than sum of reference DC capacitor voltage and real power difference in step load changes.

The switching frequency of the controlled switches has a large impact on source current THD. The higher is the switching frequency, the lower is the THD of source current. To compensate a particular harmonic, the switching frequency must be higher than 10 times of that harmonic frequency. To compensate up to 20^{th} harmonic, the switching frequency required is $20*10*50=10kHz$. But if the purpose is only to compensate the reactive power without considering harmonics, one can switch at a frequency of 500 Hz.

1.2. Literature review on control strategies applied to shunt Active Power Filter and other power electronic circuits

As discussed before APF can perform many simultaneous work due to the closed loop switching control application. Therefore the study of control strategies of APF is very important. APF control techniques mainly divided into three categories, such as:

- Control of DC capacitor voltage along with generation of reference source current
- Switching scheme
- Current control of APF

1.2.1. Control of DC capacitor voltage along with generation of reference source current

Mostly a Proportional- Integral (PI) controller is used to control the DC link capacitor voltage as well as to estimate peak value of reference source current for both single phase and three phase APF [1-4]. The output of PI controller is multiplied with unit vector of source voltage to generate reference source current. Unit vector implies a sine wave having unit peak value with phase same that of source voltage. As PI controller has large impact on source current harmonics, a low pass filter is connected at the output of PI controller to reduce the source current THD. Some advance technologies, such as fuzzy logic, artificial neural network (ANN) and genetic algorithm

has been used in [40-44] to generate reference source current. In [45] P. Kumar and A. Mahajan compared different soft computing techniques for generating reference source current. They found that APF give very good response under frequent load variation by application of soft computing techniques. In [48] comparison of PI controller and fuzzy logic controller has been carried out for controlling the DC voltage of capacitor. The generation of reference current using the combination of ANN and fuzzy logic is explained in [46]. In this literature all the analysis are done in discrete time domain. The main benefit of this controller is that it can handle nonlinearity. In [15], harmonics are estimated using neural network and real power loss by circuit elements of APF is estimated using PI controller. Both PI controller and neural network are used to generate reference source current. A three phase shunt active power filter was proposed by H. Akagi using instantaneous active and reactive power theory [49]. In this control strategy, reference source currents are calculated instantaneously using instantaneous source voltages and load currents. Further development in this strategy was done by S. Bhattacharya, who calculated *d-q (direct-quadratic)* components of instantaneous three phase currents [50]. This paper gives concept about synchronous reference frame and the procedure to calculate reference source current instantaneously without sensing the source voltage. In [52], a modified reference current extraction method is proposed using both *p-q(active –reactive)* and *d-q* theory . In [5], reference source current is calculated using real power balance of the system. The peak value of source current required to balance the real power loss of the circuit elements is calculated. The peak value of source current required to provide real power to nonlinear load is also calculated. Finally both the peak values are added to give the peak value of reference source current.

1.2.2. Switching scheme

Modulation scheme plays an important role in reducing the source current THD. Mostly two types of switching modulation schemes are applied to active power filter, hysteresis modulation (HM) and pulse width modulation (PWM). But for a single phase APF both HM and PWM switching schemes are further classified into two types, unipolar modulation and bipolar modulation. In [13] unipolar PWM based switching scheme is applied, whereas in [29] bipolar PWM based switching scheme is applied. Similarly unipolar hysteresis modulation based switching scheme is applied in [3], whereas bipolar hysteresis modulation scheme is applied in [2]. A brief description of unipolar and bipolar modulation schemes is given below. As shown in

Fig. 1.6 for positive source current, unipolar modulation employs $+V$ and 0, and for negative source current it employs $-V$ and 0. But bipolar modulation scheme only employs $+V$ and $-V$ both for positive and negative current.

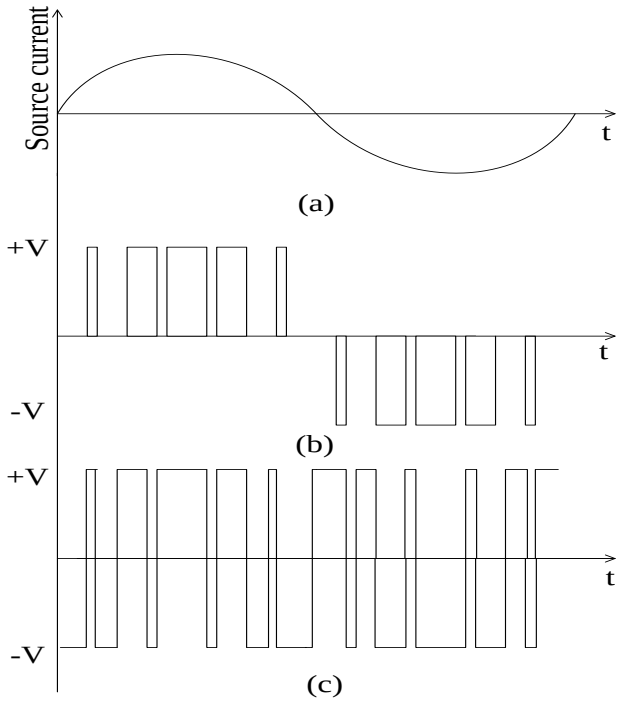

Fig. 1.6 Switching scheme. (a) Source current, (b) Unipolar Modulation, (c) Bipolar Modulation

In unipolar modulation, even harmonics are found to be absent, so THD of source current in bipolar modulation is twice that of unipolar modulation scheme. In PWM switching scheme, switching frequency remains constant, where as in HM switching scheme, switching frequency may varies as the load changes. To control the switching frequency, an adaptive hysteresis band based current controller for APF is presented in [53]. In this control strategy hysteresis band width changes with change of load. But it requires complicated mathematical calculations. B. Mazari proposed a method of updating hysteresis band using fuzzy logic to avoid mathematical calculation [55]. All the above discussed hysteresis band controllers are based on two level hysteresis band. In [54] a three level hysteresis band based current controller is presented. THD of source current reduced significantly in three level hysteresis band based controller of APF.

1.2.3. Current control of APF

Although most of the research on APF is based on reference current extraction method and switching schemes, current control of APF also plays a significant part in analyzing stability of the complete system, providing robustness under external disturbances and reducing THD of the source current. Current of APF can be controlled directly or indirectly. In direct current control method, the sensed coupling inductor current used directly in the controller of APF. In indirect current control method sensed source current is used in the controller to generate switching pulses. In [1-3], [6] and [38] indirect current controller is implemented, whereas [4] and [15] are based on direct current controller. Mostly indirect current control techniques are applied as it is easier to implement. A resonant current controller is presented in [6]. A Lyapunov stability based current control strategy is presented in [4]. The concept of equilibrium points and linearization of single phase shunt APF is explained in literature [29]. Both model reference adaptive current controller [29], Lyapunov based current controller [4] are very good method for analyzing stability of the system. It is noticed that transient response of the system is significantly improved in [29]. The sliding mode (SM) control is applied to three phase shunt APF in [38]. Also in both literature [1] and [2] SM current control strategy is applied to single phase shunt APF. SM controller via feedback linearization is applied to shunt APF in [3]. Coming into the SM current control strategy and feedback linearization based current control strategy, it is found that these two control strategies are frequently applied to improve the performance of other power electronics devices.

To avoid the drawbacks of variable switching frequency, a PWM based constant switching frequency SM controller of DC-DC converter is reported in [10]. Similarly fixed switched frequency SM controller for single phase VSI is developed in [13]. To make the boost converter robust under variation of input voltage and load, an adaptive SM controller is presented in [56]. A variable sliding surface based position control of DC motor is presented in [58]. Maximum power point tracking method of photovoltaic system using SM controller is analyzed in [57]. In this paper instead of sensing voltage of the capacitor connected across the photovoltaic system, current flowing through the capacitor is used in the SM controller. In [59], dynamic stability of the photovoltaic system connected to grid is analyzed using zero dynamic of the system. This process is nothing but the feedback linearization of grid connected photovoltaic system. A robust Partial Feedback Linearization (PFL) scheme of the photovoltaic system for maximum power point

tracking is presented in [60]. This control algorithm is mainly robust under parameter uncertainties. Also an Exact Feedback Linearization (EFL) based controller design of boost converter is reported in [30]. The complete description of SM control strategy is explained in [11]. Similarly a detail explanation of feedback linearization method is given in [34]. A brief explanation of both SM control method and feedback linearization control method is given below.

1.2.3.1. Sliding mode control

SM control is one of the nonlinear control strategy. It is mostly applied to variable structure system. The basic principle for applying SM control strategy is to design a sliding surface or switching function. Then the switches of power electronic device are controlled in such a way that the system trajectory will be directed towards the sliding surface, slides along the surface and eventually reach the equilibrium point. More detail about equilibrium point is given in [29]. The system performance depends on the design of sliding surface. In [10], the sliding surface taken is given by

$$S = \alpha_1 p_1 + \alpha_2 p_2 + \alpha_3 p_3 \tag{1.4}$$

Where $\alpha_1, \alpha_2, \alpha_3$ are positive constant and p_1, p_2, p_3 are state variable of the DC-DC converter. In [12] the sliding surface taken is given by

$$S = (\frac{d}{dt} + \rho)(\mathrm{x} - \mathrm{x}_d) \tag{1.5}$$

Where ρ is a positive constant and $\mathrm{x} - \mathrm{x}_d$ is the error between state variable to be controlled and desired reference variable. After designing of the sliding surface, the next step is to define a control law based on three conditions. These conditions are given as follows:

(1) Reaching condition or hitting condition
(2) Existence condition
(3) Stability condition

The aim of reaching condition is that regard less of initial position, the trajectory of the system will be directed toward the sliding surface. Once it reaches the sliding surface, to maintain the trajectory on the surface is the objective of existence condition. The existence condition can be

treated as local reachability condition. As shown in Fig. 1.7 (E) the trajectory reaches the sliding regime at point (a), slides along the surface (existence condition) and finally settles at the equilibrium point. The inequality which makes the system satisfy the reaching and existence condition is given as follows:

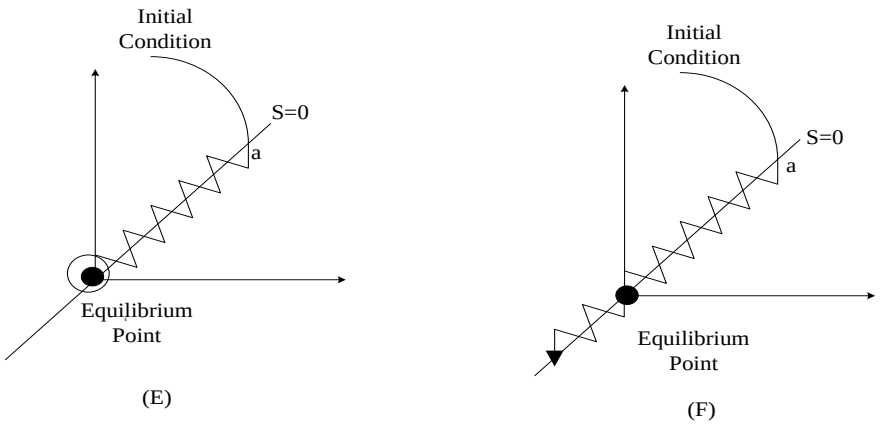

Fig. 1.7 Sliding conditions (E) stable system (F) unstable system

$$\lim_{S\to 0} S.\frac{dS}{dt} < 0 \tag{1.6}$$

The above inequality is based on lyapunov stability theorem, of which the lyapunov energy like function is

$$V(S) = \frac{1}{2}S^2 \tag{1.7}$$

The stability condition is for ensuring system trajectory to reach the equilibrium point and to settle there for the rest of the time. The sliding coefficients must be chosen carefully to ensure the stability of the system. As shown in Fig. 1.6 for a stable system the system trajectory slides along the surface and finally settles at the equilibrium point. But for an unstable system the trajectory crosses the equilibrium point and move towards infinity.

1.2.3.2. Feedback linearization control

This is also one of the nonlinear control strategy, in which the nonlinear dynamics of the system is transformed into a linear dynamics and then linear control methods are applied to control the complete nonlinear system. This linearization method is better than the conventional Jacobian linearization method as there is no approximation of the dynamics took place in the linearization

process. Feedback linearization of a system can be done by two different methods, input-state linearization and input-output linearization.

All the nonlinear systems are not input-state linearizable. Diffeomorphism condition must be satisfied for a system to be input- state linearizable. Diffeomorphism in detail is explained in [61]. Sometimes even state equations are completely linearizable, the controllability of the system becomes difficult as the output variable to be controlled takes complicated form by state co-ordinate transformation. In this case better controllability can be achieved by input-output linearization. All the dynamics of the nonlinear system may not be taken into consideration in input-output feedback linearization. Sometimes some dynamics remain unobservable in input-output linearization. These dynamics are known as internal dynamics of the system. Stability of the internal dynamics must be checked to know about stability of the complete system. In general three steps must be followed in input- output linearization. These steps are given below:

- Differentiate the output until input appears in the output equation
- Choose input considering the stability of the system, so that it can cancel the nonlinearity
- Check the stability of the internal dynamics of the system

Relative degree of a system plays a vital role in input- output linearization method. Relative degree of a system is defined as the no of times the output of a system to be differentiated, for the input to appear in the output equation. The nonlinear system have internal dynamics, when the relative degree of a system is less than the order of the system. The conclusion about stability of the internal dynamics can be obtained by considering the zero dynamics of the system. The zero dynamics is nothing but the internal dynamic of the nonlinear system when the output of the system is made zero by the input of the system. The nonlinear system can also be said partially linearizable when part of the system dynamics remains unobservable. This is the case for consideration of stability of internal dynamics. But by use of Tellegen's theorem the system can be exact feedback linearizable and there is no need to consider internal dynamic stability. More about Tellegen's theorem is explained in [3]. Lie derivative is the mathematical term generally used in feedback linearization process for calculation of relative degree and control input co-ordinate transformation, etc. in latter chapters lie derivative is used for related calculation in feedback linearization process.

1.3. Research motivation

From the review made, the following points are observed and motivate for further consideration.

- In general unit vector of source voltage is used in the reference current extraction process. This is why the APF source current THD increases to an unacceptable level as the source voltage THD increases. So it is required to make reference source current THD independent of source voltage THD.
- Dynamic response of the system improves by separating harmonic extraction circuit from filter capacitor voltage controller.
- As high and varying switching frequency causes switching losses, conduction loses and even damage of the system, it is required to keep the switching frequency constant.
- Sliding mode (SM) control is well known due to its ease of implementation and robustness.
- Feedback linearization based controller improves the performance of power electronic systems by analyzing stability of the complete system.
- The literatures connected to PFL based control technique reveals benefits of applying of PFL based control techniques over EFL based control technique. Therefore it is required to apply PFL based control technique to shunt APF and performance should be compared with EFL based control technique.

1.4. Thesis objective

The objectives of the thesis sare as follows:

- To develop an analog SM controller for APF to reduce steady state current error and to make source current THD independent of Source voltage THD by use of band pass filter.
- To present Multisim simulation results for showing the method of analog low cost implementation.
- To design a PWM based constant switching frequency SM controller for single phase shunt APF.
- To generate the reference source current combining both ANN based modified extraction circuit and PD controller.

- To apply PFL control technique to single phase shunt APF using averaged dynamic model of APF.
- To develop an experimental prototype of PFL technique based single phase shunt APF using dSPACE 1104.
- To extend the application of proposed PFL technique to three phase APF.
- To validate the theory of proposed control strategies using MATLAB/Simulink.

1.5. Thesis organization

The thesis consists of six chapters, these are organized as follows:

Chapter 1 covers the introductory concepts of nonlinear load, harmonics, and APF. Literature review on reference source current generation methods, switching schemes, and current control techniques of shunt APF is explained in detail in this chapter. A brief introduction of feedback linearization control and SM control is also given. Eventually motivation, objective and organization of the thesis is reported.

Chapter 2 presents a low cost analog SM controlled single phase shunt APF. In this control strategy, THD of source current becomes independent of source voltage THD by use of band pass filter. MATLAB/Simulation results are presented to check the performance of integral SM current controller and band pass filter based reference current generation method. Finally Multisim simulation diagram and simulation results are presented to reveal low cost analog implementation methods.

Chapter 3 presents a constant frequency SM controller for shunt APF. Combined control strategy using ANN based fundamental source current extraction circuit and PD controller is used for reference source current calculation. Reference current extraction method is explained properly and finally MATLAB/Simulink simulation results are presented to validate the theory.

Chapter 4 presents the application of PFL control techniques to single phase shunt APF. The internal dynamics stability is analyzed in this chapter. The switching scheme used in [3] is explained. MATLAB simulation results are presented to reveal the effectiveness of theory. Finally an experimental prototype of the proposed method is developed using dSPACE 1104. Experimental results are also presented.

Chapter 5 presents the extension of proposed PFL technique in chapter 4 to three phase shunt APF. Evaluation of this control strategy is done using MATLAB/Simulink software.

Chapter 6 focuses on the conclusory remarks of this thesis. It also suggests some future directions of this research work.

CHAPTER 2

DESIGN OF AN ANALOG SLIDING MODE CONTROLLER FOR SINGLE PHASE SHUNT ACTIVE POWER FILTER

2.1. Introduction

From the literature review made on active power filter , it is clear that a lot of active power filtering methods have been proposed in the literatures to reduce THD of source current and to improve the power factor on the electrical network. But most of the control strategies are based on some advance technologies such as fuzzy logic, neural network and genetic algorithm. These control strategies gives high performance and flexible designs. But the cost of implementation of these control algorithms is very high.

To reduce the cost of implementation some analog control implementations have also been evaluated in the literature [1], [4], [14]. These controllers provide good performance at nominal source conditions. However, in distorted sources, additional analog circuitry is required to fulfill the expected features. Considering these problems, this chapter reports a SM controlled active filter, which is applicable under both nominal source and distorted source.

2.2. Chapter objectives

The main goal of this chapter is to design a low cost active filter with low THD and high robustness under external disturbances. A band pass filter is used in the generation of reference source current, which makes active power filter to be applicable for both nominal source and distorted source. An integral sliding surface is chosen to reduce the steady state current error. Unipolar hysteresis modulation switching scheme is chosen to get the desired active power filter performance. A complete analysis of sliding mode control theory is given and MATLAB/Simulink based simulation results are reported to verify the theory. LABVIEW (Multisim) based simulation circuits and corresponding results are also presented to report the low cost design method.

2.3. Dynamic model of single phase shunt APF

In this section dynamic model a single phase shunt APF as shown in Fig. 1.4 is reported. The filter capacitor voltage (V_C) must be maintained at a high value than the peak of the ac source in order to shape inductor current (I_L) as required at any instant point in the line cycle. During the positive half cycle of the source voltage, I_L can be made more positive by making $v_x = 0$ and I_L can be driven toward zero by making $v_x = V_C$. During negative half cycle of the source voltage, I_L can be made more negative by making $v_x = 0$ and I_L can be driven toward zero by making $v_x = -V_C$ [1]. In order to analyze the operation mode of the APF, we define the switching function $U_i = 1$ if T_i is ON and $U_i = 0$ if T_i is OFF, where $i = 1, 2, 3, 4$ denoting the switch number. Here we note two switches from the same inverter leg must operate complementary. This gives

$$U_1 + U_2 = 1 \text{ and } U_3 + U_4 = 1 \tag{2.1}$$

Also:

$$v_x = (U_1 U_4 - U_2 U_3) V_C \tag{2.2}$$

Using (2.1) and (2.2) one gets

$$v_x = (U_1 + U_4 - 1) V_C \tag{2.3}$$

The current flowing through filter capacitor (I_C) can be expressed as:

$$I_C = (U_1 + U_4 - 1) I_L \tag{2.4}$$

With analytic expressions of v_X and I_C, the dynamic state equations for the inductor current and capacitor voltage are as follows:

$$L \frac{dI_L}{dt} = V_S - I_L R - (U_1 + U_4 - 1) V_C \tag{2.5}$$

$$C \frac{dV_C}{dt} = (U_1 + U_4 - 1) I_L \tag{2.6}$$

where V_S is the source voltage.

Assuming $U_1 + U_4 - 1$ as U, the state dynamic model of shunt APF becomes:

$$\frac{dI_L}{dt} = \frac{1}{L}(V_S - I_L R - V_C U) \tag{2.7}$$

$$\frac{dV_C}{dt} = \frac{1}{C}(I_L U) \tag{2.8}$$

2.4. Development of the control algorithm

This basic approach consists of two control loops. Outer voltage loop regulates the capacitor voltage and inner current loop tracks the reference current signal. PI controller is used to control the DC side capacitor voltage. Inductor current is controlled using SM control strategy.

2.4.1. Sliding mode current control of APF

In order to improve the performance of the controller, in this chapter a control mode is proposed based on sliding surface which involves source current (I_S). Let (V_{DC}, I_S^*) be the reference values of filter capacitor voltage and source current. These reference values of filter capacitor voltage and source current are also known as equilibrium points of the system. The error function $e_1 = I_S - I_S^* = 0$ represents the sliding surface in [1] and [2]. However, in this situation the system has steady state current error. In order to reduce steady state error an integral term $e_2 = \int e_1 dt$ is introduced.

The proposed sliding surface can be written as follows:

$$S = e_1 + \lambda e_2 \tag{2.9}$$

where λ is a control parameter known as sliding coefficient. Positive value sliding surface coefficients λ ensures the stability of the APF. As explained before the existence condition

Table 2.1

Switching scheme used in analog SM controller

	$V_S > 0$	$V_S < 0$		$S > 0$	$S < 0$
U_3	0	1	U_1	1	0
U_4	1	0	U_2	0	1

$\lim_{S\to 0} S.\dot{S} < 0$ must be satisfied to bring the dynamics of the system on to sliding surface and to maintain it on the surface. In SM controller in order to satisfy the existence condition we usually determine U as following:

$$U = \begin{cases} 1 & if \quad S>0 \\ 0 & if \quad S=0 \\ -1 & if \quad S<0 \end{cases} \tag{2.10}$$

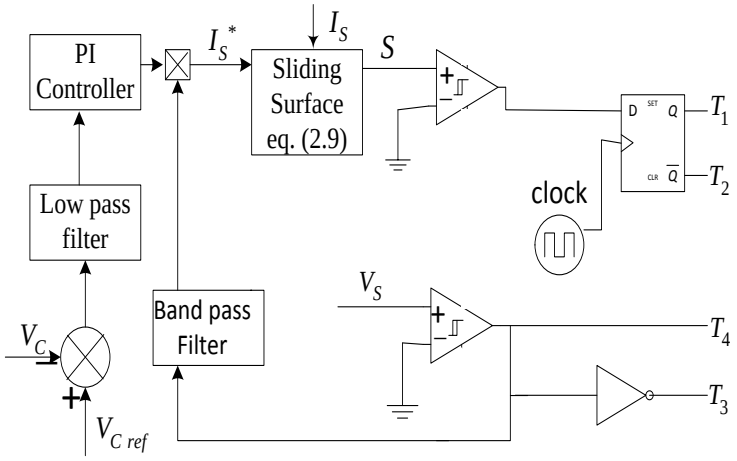

Fig.2.1 Analog sliding mode controller for shunt APF

The sign of $\dot{S}$ should be controlled to satisfy the existence condition. This can happen by application of control law defined in (2.10). A unipolar HM based switching scheme is applied to implement the proposed SM control strategy. The applied switching scheme is shown in Table 2.1. Switches of one leg of the APF (T_3, T_4) operate at source voltage frequency and that of other leg (T_1, T_2) operate at high frequency. For $V_S > 0$ (T_4 is ON), if T_1 is ON, the state variable trajectory S increases ($\dot{S} > 0$) and becomes positive. If T_1 is OFF, S decreases ($\dot{S} < 0$). For $V_S < 0$, the situation is similar. Switches T_3 and T_4 are used to force $v_x \le 0$ and $v_x \ge 0$ respectively, while Switches T_1 and T_2 are used to actively shape I_L. The control law U makes the state trajectory to reach the sliding surface in finite time, and then slides along the surface toward equilibrium point exponentially. The complete analog SM controller for single phase shunt APF is shown in Fig. 2.1.

With the proposed controller switching frequency varies during the source period, due to the inherent behavior of the sliding mode control. The maximum frequency is expected at zero voltage crossing points and the minimum frequency is obtained at peak source voltage values. In the proposed controller the maximum switching frequency $f_{S\ MAX}$ is fixed by using D flip flop at the output of the comparator. Note that maximum switching frequency is always one-half of the clock/decision frequency. One benefit of constant decision frequency is that the maximum switching frequency of the switches is bounded.

2.4.2. Reference source current calculation

Fundamental component of the gate pulses to switch T_4 is in same phase to that of source voltage (V_S). So a band pass filter can be used to generate the fundamental component of gate pulse by filtering its harmonics. The characteristics of bandpass filter have a significant effect on the active power filter performance. The bandwidth should be small enough to sufficiently attenuate the harmonic components of the reference current.

The capacitor voltage is put through a RC lowpass filter which yields the average capacitor voltage. This quantity is compared to the reference capacitor voltage, with the difference driving the PI controller. The output of the PI controller is a slow varying variable. This is the peak value of reference source current. This implies that the output of PI controller gives sum of peak value of fundamental load current and the peak value of source current required to compensate the real power loss in filter capacitor. As a result this slow varying variable is multiplied with the output of band pass filter to generate the desired reference source current.

As band pass filter is used to calculate reference current, small variation in amplitude of source voltage does not affect reference source current. This is why this active filter is applicable for both distorted and nominal source.

2.5. MATLAB/Simulink based simulation results

To check the robustness and effectiveness of the proposed analog SM controller, the complete shunt APF system is simulated using MATLAB/Simulink. The nonlinear load used is a diode bridge rectifier having 500-μF capacitor in parallel with a 45-Ω resistor at its output side. The system parameters used in the simulation are given in Table 2.2. Cutoff frequency of RC

lowpass filter has been set as 80 Hz. Cutoff frequency and bandwidth of bandpass filter have been set as 50 Hz and 6 Hz respectively.

Table 2.2

System parameters used for MATLAB/Simulation in analog SM controller

L- 5 mH	V_S^{RMS} *- 110 V*	λ *- 2000* S^{-1}
V_{Cref} *- 200 V*	f_{V_S} *- 50 Hz*	K_P - 0.5
C- 1100 µF	f_{Clock} -40 kHz	K_i -10

The THD of the source voltage under ideal condition is found to be 0.19%. Similarly the THD of the load current considering up to 30th harmonics is calculated as 82.9%. Simulated load current and source voltage waveforms are shown in Fig. 2.2. By application of proposed controller, the source current THD is reduced to 4.51%. Fig. 2.3 shows source current and source voltage waveforms of the proposed analog SM controller.

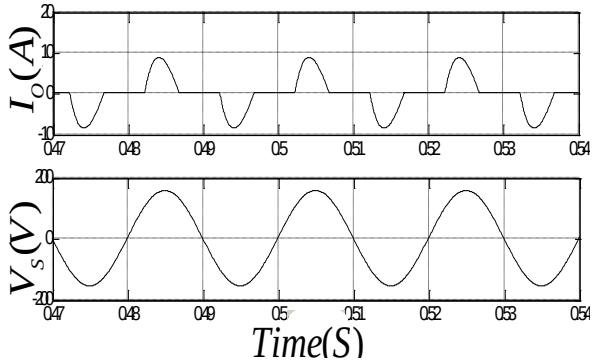

Fig. 2.2. Source voltage (bottom). Load current (top). Analog SM controller

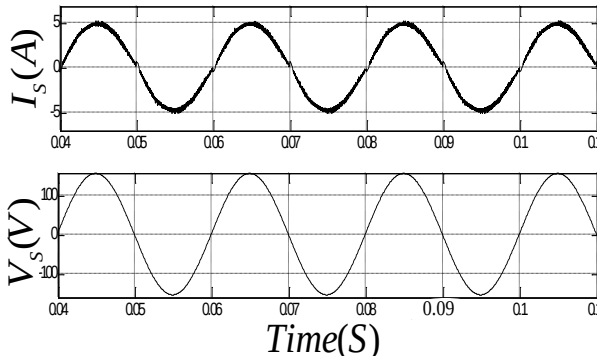

Fig. 2.3. Nominal voltage source. Source voltage (bottom). Source current (top). Analog SM controller

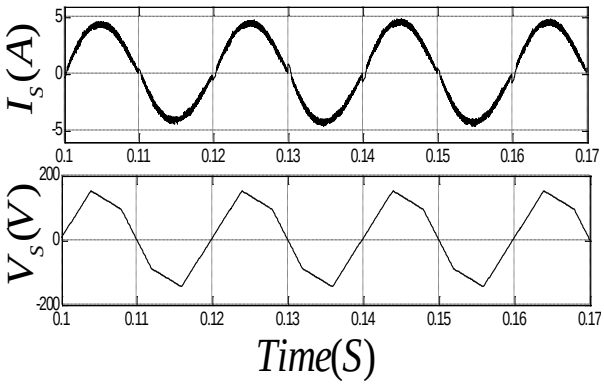

Fig. 2.4. Distorted voltage source. Source current (top). Source voltage (bottom). Analog SM controller

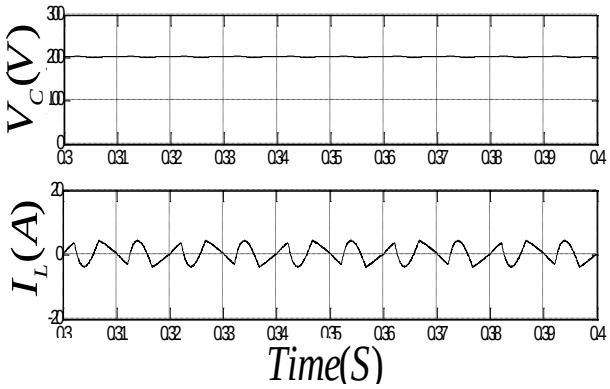

Fig. 2.5.Filter Capacitor voltage (top). Inductor current (bottom). Analog SM controller

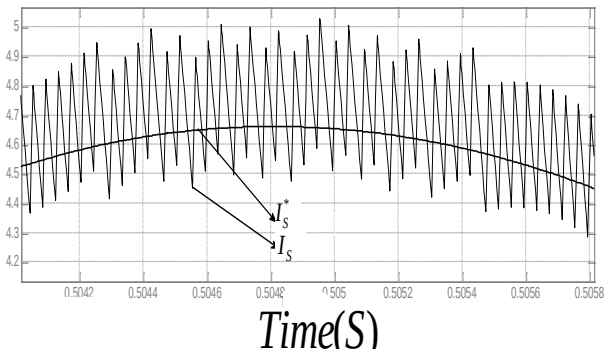

Fig. 2.6.Source current (I_S) and reference Source current (I_{Sref}) with sliding surface $S = e_1 = I_S - I_{S\,ref}$

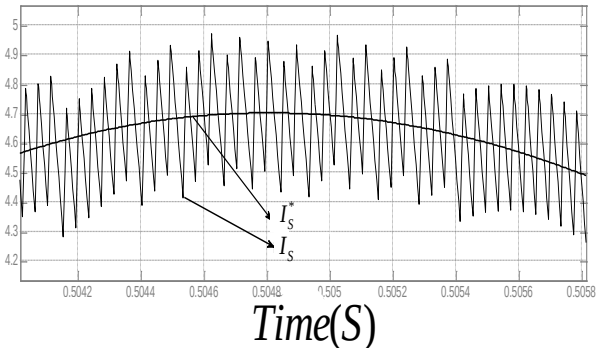

Fig. 2.7.Source current (I_S) and reference Source current (I_{Sref}) with sliding surface $S = e_1 + \lambda e_2$

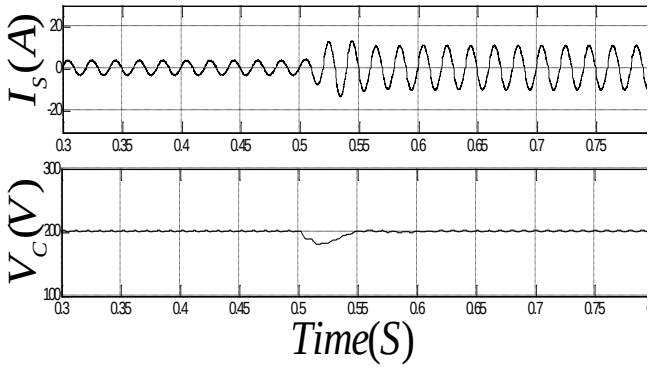

Fig. 2.8. Filter capacitor voltage (bottom). Source current (top), Dynamic response for step load change

In practical application, the source voltage waveform is normally distorted. To check the performance of the proposed controller in such situation, a distorted source voltage with a THD 10.32% has been employed. The waveforms of source current for distorted source is shown in Fig.2.4 and THD of source current under this condition is calculated as 4.93%. It is clear that source current THD is almost independent of source voltage THD.

The actual source current (I_S) and reference source current (I_S^*) for sliding surfaces without integral term and with integral term are shown in Fig. 2.6 and Fig.2.7 respectively. It is observed that there is reduction in steady state current error by introduction of integral term in the sliding surface. After looking at Fig. 2.5, it is observed that the filter capacitor voltage is maintained approximately at required constant voltage of 200 volts. Also Fig. 2.5 shows inductor

current waveforms. This inductor current is equal to sum of all the harmonics present in load current but with opposite polarity.

The dynamic response of the proposed analog SM controller is checked by changing the load suddenly. Fig. 2.8 shows the transient response of the source current and capacitor voltage of the proposed controller. It is noticed that a small deviation from steady state value is occurred during step load change and time taken to settle is also very small.

2.6. MULTISIM based simulation results

The complete schematic of low cost analog SM controlled shunt APF is shown in Fig. 2.9. Multisim based circuit simulation diagram shows the method of low cost implementation of proposed controller. As shown in Fig. 2.9, a 20:1 transformer and a voltage controlled voltage source are used for sensing the source voltage and voltage of the filter capacitor respectively. The sensed filter capacitor voltage is passed through a RC lowpass filter to reduce source current THD. The output of lowpass filter is fed through a difference amplifier with unit gain to get the error between filter capacitor voltage and its reference value. This error output is fed to a PI controller, which comprises of three operational amplifier. Out of three operational amplifiers two are used for providing proportional gain and integral gain and the other is a summing amplifier. The output of PI controller is multiplied with the output of bandpass filter by a multiplier (part number AD633AN) to generate the reference source current. Suitable resistances are connected at the output of the multiplier to give the proper multiplication of the inputs as per datasheet specifications of AD633AN. A Junction Field Effect Transistor (JFET) based operational amplifier (part number TL084CN) is used in PI controller, bandpass filter and all other arithmetic operation. The sliding surface is also developed by using operational amplifiers as per the theory. A high frequency comparator (part number LM 710AMJ) is used for generating gate pulses of APF. Two comparators are used in the controller. The output of one comparator is connected to a NOT gate (part number 4009BD_5V) to provide inverting gate pulses to one leg of the APF. The other leg of the APF is operated at high switching frequency to maintain the required sliding surface trajectory. As explained before the switching frequency of the proposed APF is controlled by a D flipflop (part number 74LS74D). This fliflop integrated circuit comprises of two D flipflops. Out of these two D flipflops only one is used in the proposed controller. The present and clear input of D flipflop is connected to ground.

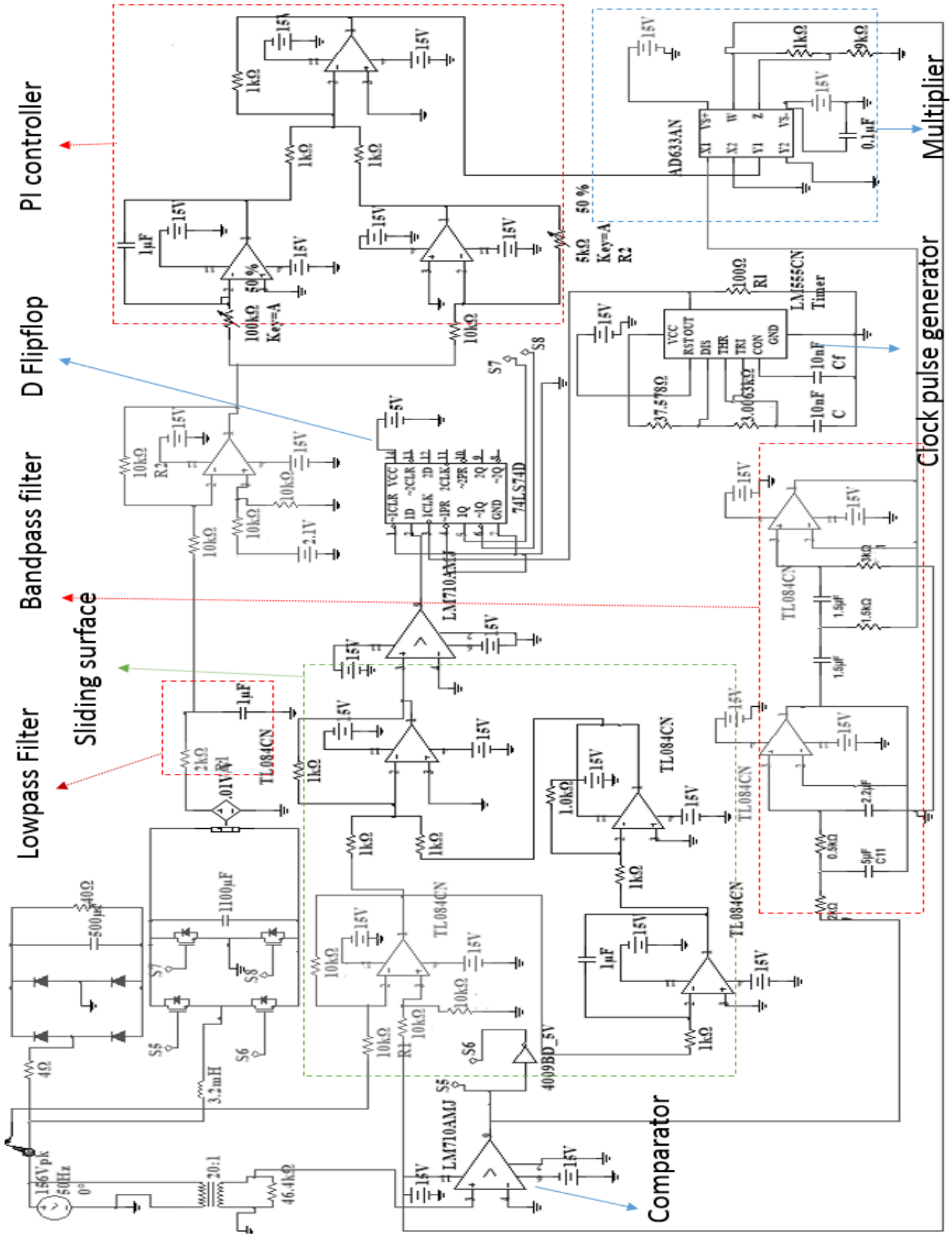

Fig. 2.9. The schematic of analog SM controller for shunt APF

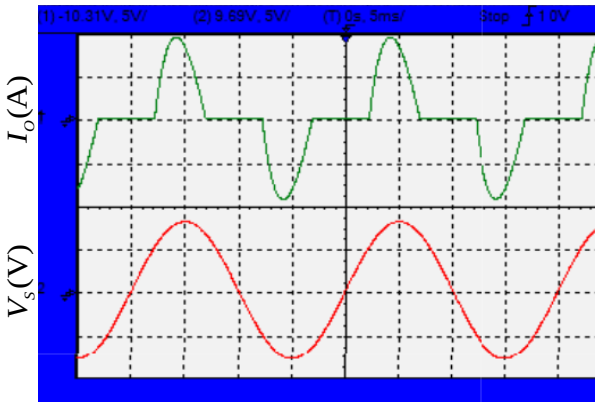

Fig. 2. 10. Multisim based simulation results. Nominal source. Source voltage (bottom). Load current (top). Analog SM controller

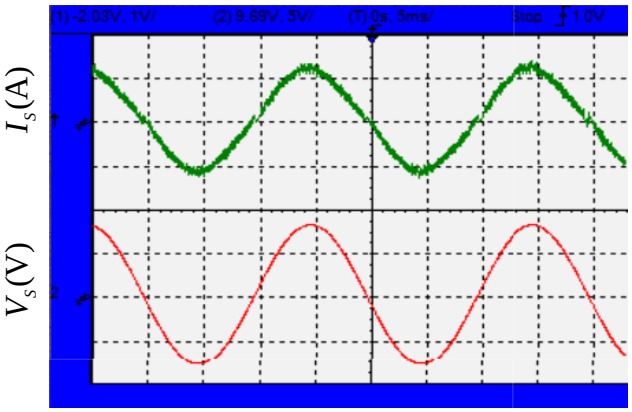

Fig. 2. 11. Multisim based simulation results. Nominal source. Source voltage (bottom). Source current (top). Analog SM controller

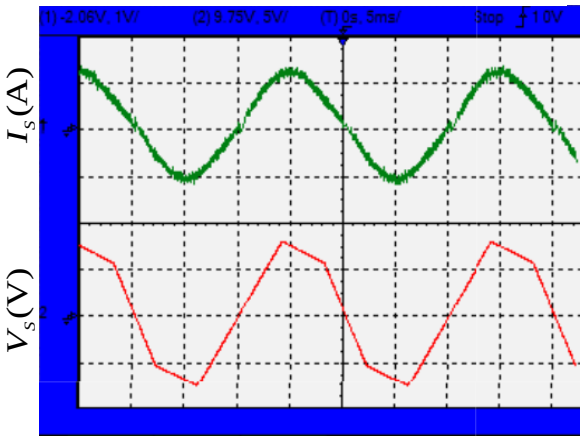

Fig. 2. 12. Multisim based simulation results. Distorted source. Source voltage (bottom). Source current (top). Analog SM controller

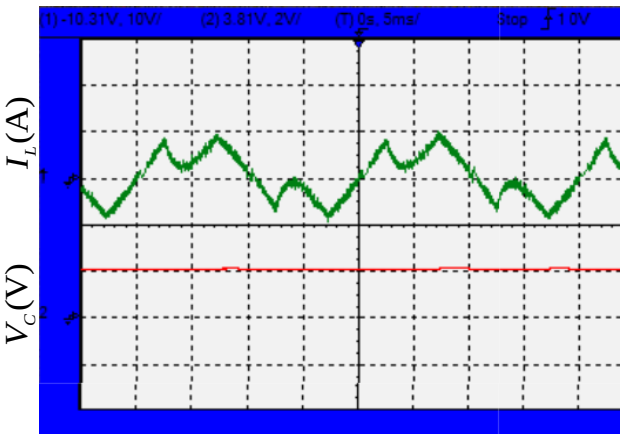

Fig. 2. 13. Multisim based simulation results. Nominal source. Filter capacitor voltage (bottom). Inductor current (top). Analog SM controller

The clock pulse to the D flipflop is generated by LM 555 timer. The frequency of the clock pulse is determined by the resistance values connected to LM 555 timer. The bandpass filter circuit and the clock pulse generator circuit are made by the application of Multisim circuit wizards. Circuit wizard is one of the tools of Multisim circuit simulation platform for making some popular circuits such as filter, timer, adder, etc. All the integrated circuits are given proper supply voltages as per their data sheet specifications. At first, all the components used in the controller are checked separately for conformation regarding their working nature. Then they are used in the proposed controller. The total cost of all the components used in the analog sliding mode controller is within one thousand rupees. Thus, the practical implementation cost of the proposed controller is very cheap.

Fig. 2.10 shows Multisim based simulation results of source voltage and load current for the nonlinear load as shown in Fig. 2.9. After implementing the proposed controller using anlog integrated circuits in Multisim platform, the resulting source voltage and source current waveforms are shown in Fig. 2.11. Source current is found to be approximately sinusoidal and in same phase to that of source voltage. This conforms the appropriateness of the Multisim implemented simulation circuit of the proposed controller. The source voltage and source current waveforms for distorted source condition is shown in Fig. 2.12. Source current waveforms are found sinusoidal and independent of source voltage waveforms. This verifies that bandpass filter, designed by Multisim circuit wizard tool is working properly. Finally in Fig. 2.13 the filter capacitor voltage and inductor current are shown.

2.7. Chapter summary

In this chapter a modified low cost analog SM controller for single phase shunt APF is presented. Basically two modifications have been carried out. One is the introduction of integral term in the sliding surface and another is the application of bandpass filter in the reference current generation process. A brief explanation of SM current controller of APF and reference current generation method is reported. It is noticed from MATLAB/Simulink based simulation results that introduction of bandpass filter in the reference current calculation method of APF makes THD of source current independent of THD of source voltage. MATLAB/Simulink based simulation results also verifies the reduction of steady state current error due to introduction of integral term in the sliding surface design. Finally the analog implementation of proposed controller is carried out in Mulisim circuit simulation platform. The schematic of the complete APF is presented to report the low cost implementation of the proposed controller. A brief explanation of Multisim based simulation process is reported and simulation results are also presented.

CHAPTER 3

A CONSTANT SWITCHING FREQUENCY ADAPTIVE SLIDING MODE CONTROL DESIGN FOR SHUNT ACTIVE POWER FILTER SYSTEM

3.1. Introduction

As per the discussion in the previous chapters, SM control is well known due to its ease of implementation and robustness. SM controllers have a property of operating at infinite and varying switching frequency such that the state variables of the system follow the required trajectory. However high and varying switching frequency causes losses and even damage of the system. Various techniques have been proposed in sliding mode controlled APFs to control the switching frequency [1]-[3]. These are mainly based on hysteresis modulation. So the maximum switching frequency can only be controlled in these control strategies. But in PWM based SM controller of any system, the switching frequency remains constant.

From the literature review, it has been found that APF control techniques mainly divided into two categories such as current control of APF and control of filter capacitor voltage along with generation of reference source current. A PI controller can be used to control the filter capacitor voltage as well as to generate the reference source current. The output of the PI controller gives the peak value of the reference source current. The peak value of source current depends on the load current harmonics and real power loss in the APF circuit. By making harmonics extraction method separate from the estimation of real power loss in the APF, the transient response of the complete APF system will be improved. Artificial Neural Network (ANN) can be used to extract the load current harmonics. By the application of ANN, the APF becomes adaptive to various load currents and source voltages. The weight update method plays a vital role in ANN to extract the source current harmonics. By adapting suitable weight update technique, the extraction of load current harmonics as well as the transient response can be made further faster. The use of Phase Locked Loop (PLL) in deriving the unit vector of source voltage makes APF applicable under both nominal source and distorted source.

3.2. Chapter objectives

The main focus of this chapter is to design and simulate a fixed switching frequency PWM based adaptive sliding mode current control for single phase shunt APF. ANN based modified control strategy is being used to control the DC capacitor voltage as well as to generate reference source current. The instantaneous phase of the source voltage is extracted by a phase locked loop. The same phase is used by ANN for calculating the reference source current. The application of ANN and PLL enhances the source current convergence rate of APF and also makes it adaptive under variable load and source conditions. This proposed APF is applicable under both nominal and distorted voltage source. The complete non-linear system is analyzed and simulated using MATLAB/Simulink software. Simulation results are presented to validate the theory.

3.3. Development of the control algorithm

In this section both constant switching frequency SM current controller design and the application of ANN and PD controller for controlling the DC capacitor voltage along with calculating reference source current is described. The typical configuration of APF is considered

Table 3.1

Switching states and control input

T_1	T_4	T_2	T_3	U
ON	ON	OFF	OFF	1
OFF	OFF	ON	ON	-1
OFF	OFF	OFF	OFF	0

for analysis is shown in Fig. 1.4, which is same as that of used in chapter 1. The dynamic model of APF used for analysis is already derived in chapter 1. But for ease of understanding and for convenience, the dynamic model of shunt APF is again given below:

$$\frac{dI_L}{dt} = \frac{1}{L}(V_S - I_L R - V_C U) \tag{3.1}$$

$$\frac{dV_C}{dt} = \frac{1}{C}(I_L U) \tag{3.2}$$

For all possible values of U the switching state of shunt APF is shown in Table 3.1.

3.3.1. Fixed frequency SM current controller

As the APF system is a nonlinear system and the control of APF is completely based on control of the switches, SM control can be applied to bring the system's state trajectory onto a user defined surface called sliding surface and to maintain the trajectory on that surface for the rest of the time. To reduce steady state current error and to make the source current follow reference source current a sliding surface is defined as

$$S = e_1 + \lambda e_2 = (I_S - I_S^*) + \lambda \int (I_S - I_S^*) \tag{3.3}$$

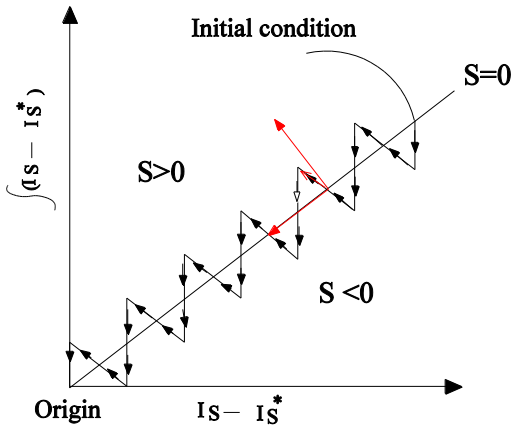

Fig. 3.1. Existence condition

After design of the sliding surface, the next important aspect is to check for existence condition for sliding mode to exist in the vicinity of the sliding surface which is possible only when the tangent to the state trajectory is made to direct towards the sliding surface. As shown in Fig. 3.1 for $S > 0$ the actual trajectory lies above the sliding surface $S = 0$. When $S > 0$, I_S is greater than I_S^*. To bring the trajectory on to the sliding surface the extra amount of current must be used to charge the capacitor. Similarly when $S < 0$ to make actual source current follow the reference source current capacitor must supply the adequate amount of current. With proper control of the switches of the APF the reaching of the trajectory on to the sliding surface and maintaining the trajectory on the surface is possible, which are known as reaching and existence of sliding mode control strategy respectively. As explained before, the SM control exists only if

local reachability condition $\lim_{S\to 0} S.\dot{S} < 0$ was satisfied. Again the discrete control law which maintains the system state trajectory on the sliding surface $S = 0$ can be expressed as

$$U = \begin{cases} 1 & if \quad S>0 \\ 0 & if \quad S=0 \\ -1 & if \quad S<0 \end{cases} \tag{3.4}$$

For ideal SM control to exist the switches of APF must be operated at infinitely high frequency. Different techniques have been applied to limit the switching frequency of the single phase APF to a maximum value in the literature [1]-[3], which causes chattering in the vicinity of the sliding surface. As shown in Fig. 3.1 the actual trajectory has two component, one is perpendicular to sliding surface and another along the sliding surface pointing towards the equilibrium point. The component along the sliding surface is responsible for both sliding motion and stability of the system. Since the movement of the trajectory is due to appropriate control of the switches, which is governed by the discrete control law as in equation (3.4), the continuous switching action responsible for horizontal component of the trajectory must lie between 0 and 1. This continuous switching action known as equivalent control input (U_{eq}) of the system, which can be found by using the condition $\dot{S} = 0$ as per literature [10].

From Fig. 1.4

$$I_S = I_L + I_O \tag{3.5}$$

Also we can write

$$I_S^* = I_L^* + I_O \tag{3.6}$$

Where I_L^* is the reference compensating current.

Considering (3.1), (3.3), (3.5) and (3.6) and making $\dot{S} = 0$ one gets

$$\frac{1}{L}\{V_S - I_L R - V_C U\} - \frac{dI_L^*}{dt} + \lambda(I_S - I_S^*) = 0 \tag{3.7}$$

From (3.7) we can obtain

$$U_{eq} = \frac{1}{V_C}\left\{V_S - I_L R - L\frac{dI_L^*}{dt} + \lambda L(I_S - I_S^*)\right\} \tag{3.8}$$

As per [2], U_{eq} is continuous and lies between 0 and 1. Considering (3.8), we obtain

$$0 < \frac{1}{V_C}\left\{V_S - I_L R - L\frac{dI_L^*}{dt} + \lambda L(I_S - I_S^*)\right\} < 1 \tag{3.9}$$

In classical PWM based APF as in [14] duty ratio (d) can be expressed as

$$d = \frac{U_{ref}}{V_{tri}} \tag{3.10}$$

Where U_{ref} is the control modulating signal and V_{tri} is the peak amplitude of triangular signal. Also ' d ' can again be expressed as

$$d = \frac{T_{ON}}{T} \tag{3.11}$$

Where T_{ON} is on time and T is total time period in which switches operates, which is constant in PWM. From (3.11) we can write

$$0 < d < 1 \tag{3.12}$$

Comparing duty ratio control of classical PWM based APF and equivalent control input of proposed SM control based APF and considering (3.9) and (3.12) and taking $V_{tri} = 1$ one can obtain

$$U_{ref} = \frac{1}{V_C}\left\{V_S - I_L R - L\frac{dI_L^*}{dt} + \lambda L(I_S - I_S^*)\right\} \tag{3.13}$$

The above calculated U_{ref} is used as modulating signal for unipolar PWM as per [12]. The switches of the APF operate at constant frequency which is nothing but the frequency of the triangular wave used as a carrier wave in unipolar PWM. The difference in PWM technique proposed in [14] and this chapter is only with the modulating control signal used for PWM.

3.3.2. Modified ANN based control strategy

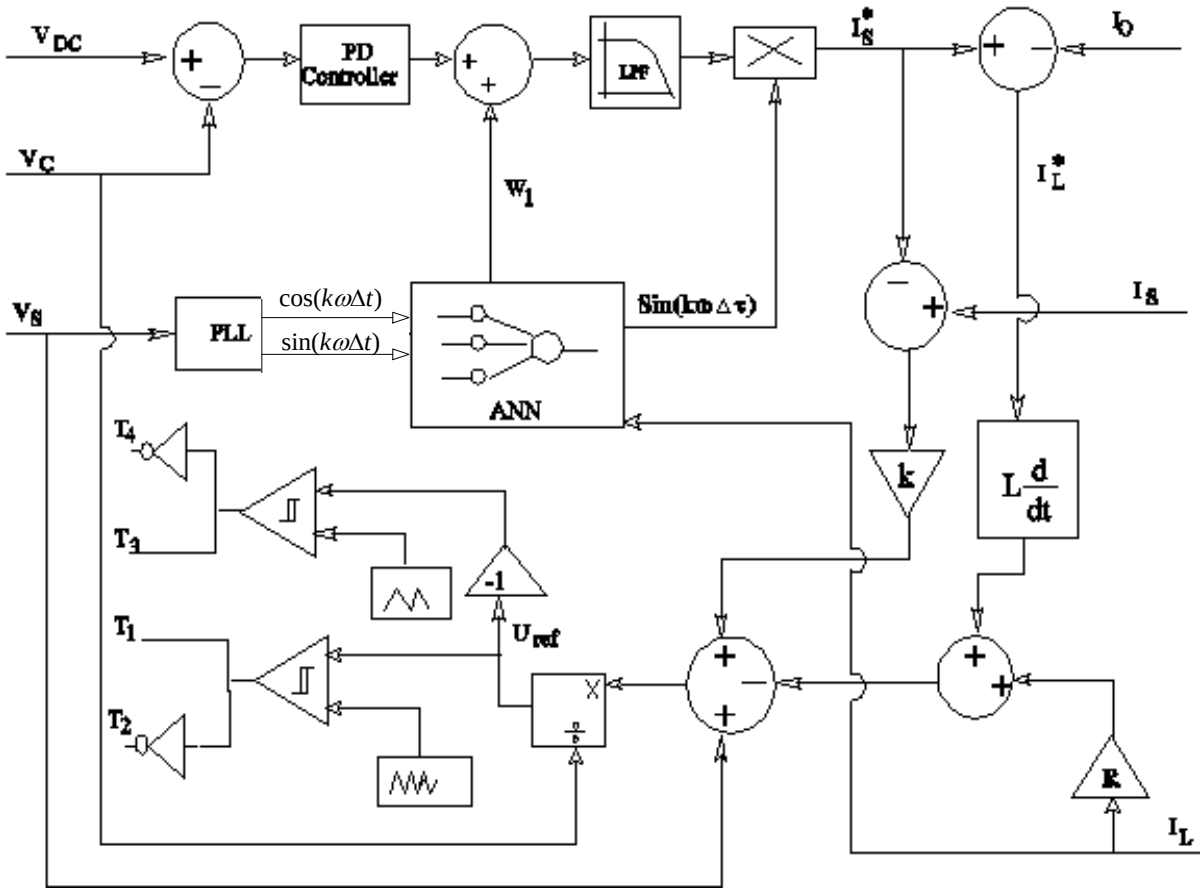

Fig.3.2. Fixed frequency adaptive sliding mode controller

The discretized instantaneous nonlinear load current can be represented by

$$I_o = \sum_{n=1}^{\infty} I_n \sin(kn\omega\Delta\tau - \theta_n) \tag{3.14}$$

where I_o is the load current, I_n is the peak value of various components of load current, θ_n is the phase angle difference between source voltage and various components of load current, $\Delta\tau$ is the discrete sampling time interval and $k\omega\Delta\tau$ is the instantaneous phase of source voltage, where $k = 0,1,2...$ The load current can be further expressed as

$$I_o = I_1 \sin(k\omega\Delta\tau)\cos(\theta_1) - I_1 \cos(k\omega\Delta\tau)\sin(\theta_1) + \sum_{n=2}^{\infty} I_n \sin(kn\omega\Delta\tau - \theta_n) \tag{3.15}$$

From (3.15) one can obtain

$$I_o = W_1^1 \sin(k\omega\Delta\tau) + W_2^1 \cos(k\omega\Delta\tau) + \sum_{n=2}^{\infty}[W_1^n \sin(nk\omega\Delta\tau) + W_2^n \cos(nk\omega\Delta\tau)] \quad (3.16)$$

Where $W_1^1, W_2^1 ... W_1^n, W_2^n$ are constants. $W_1^1 \sin(k\omega\Delta\tau)$ is the fundamental source current and $W_2^1 \cos(k\omega\Delta\tau)$ is the fundamental quadrature current, which is 90^0 out of phase to that of fundamental source current. In [8] and [13], (17) is used by ANN for extracting the fundamental source current from load current. This is a lengthy process as all $2n$ number of weights have to be updated to slow varying variables to get the fundamental source current.

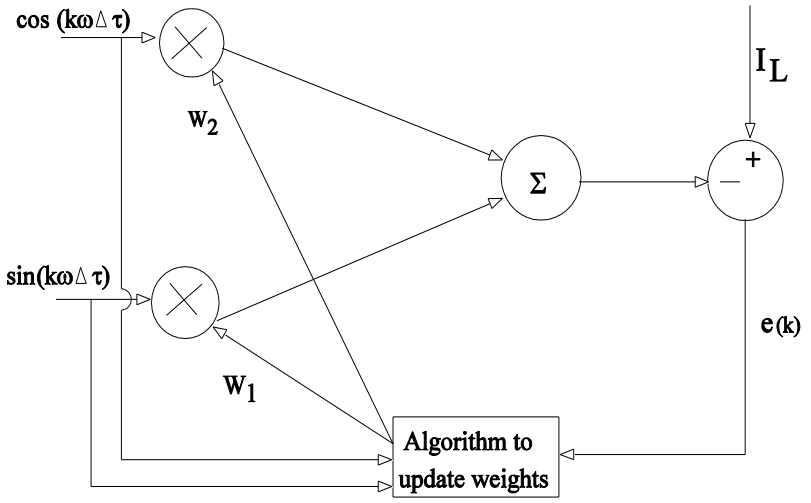

Fig.3.3. Modified ANN based extraction circuit

In this chapter modified ANN based fundamental source current extraction circuit is presented which reduces weight updating time from 2 to 3 cycle to almost half cycle of source voltage signal. Considering (3.16) one can obtain

$$I_o = W_1^1 \sin(k\omega\Delta\tau) + W_2^1 \cos(k\omega\Delta\tau) + \textit{periodic signal} \quad (3.17)$$

In this chapter instead of updating $2n$ weights only 2 weights W_1^1 and W_2^1 are updated to slow varying variables to get the fundamental source current. As shown in Fig.3.3 the input vector is taken as a matrix $X = \begin{pmatrix} \sin(k\omega\Delta\tau) \\ \cos(k\omega\Delta\tau) \end{pmatrix}$ and the weight vector is taken as a matrix $W = \begin{pmatrix} W_1^1 \\ W_2^1 \end{pmatrix}$. A

modified Widrow-Hoff delta rule based weight updating algorithm is being used to update the weights W_1^1 and W_2^1. The algorithm can be stated as follows

$$W(k+1) = W(k) + \Delta W \tag{3.18}$$

where $\Delta W = \frac{\rho e(k) X(k)}{X^T(k) X(k)}$, ρ is the learning rate which is always greater than zero.

The error between actual load current and estimated load current $e(k)$ instead of converging close to zero converges to a periodic signal almost equal to sum of all harmonic components of load current put together. As discrete sampling time interval ($\Delta\tau$) in which updating process is carried out is much less than that of period of variation of $e(k)$, updating process takes place easily. Learning rate is an important factor in the weight updating process. Lower value of learning rate takes a long time to update the weights to their desired value. While higher value of learning rate causes oscillation of the weights around their desired value. A suitable value of learning rate is chosen by taking care of amplitude of oscillation of weights and updating time.

As combination of real power loss in APF and estimation of load current harmonics is used in calculating the reference source current, real power loss in APF can be calculated separately. The peak value of the source current required to compensate the real power loss in the APF is given below [5]:

$$k_{1p} = \frac{2CfV_{DC}}{V_p} \tag{3.19}$$

Where C is the capacitance value, f is the frequency of the source voltage, V_{DC} is the reference filter capacitor voltage, and V_p is the peak value of source voltage. As derivative controller improves the transient response and reduces the peak overshoot, a Proportional-Derivative (PD) controller is used to get the peak value of source current. Proportionality gain of PD controller is set using (3.19) and derivative constant is properly adjusted by heat and trial for a better capacitor voltage regulation.The output of the PD controller gives the peak value of the filter capacitor charging current and the value of the weight W_1^1 of ANN based extraction circuit gives peak value of the fundamental source current. The peak value of the reference source current is calculated as

sum of weight W_1^1 and the output of the PD controller. The peak value of the reference source current is then passed through the low pass filter to remove the high frequency component, which helps in reducing the harmonic content in the source current. After getting reference source current SM current control strategy is being applied to control the switches of the APF.

The overall controller of the APF is shown in Fig. 3. The combination of PLL, PD controller, SM current control, ANN based extraction circuit and unipolar PWM makes the APF applicable under different load conditions and distorted voltage source with reduced harmonic content in the source current.

3.4. Result analysis

To validate the system performance overall APF model is computer simulated using MATLAB/Simulink software version 2013 (a). The solution method chosen was runga-kutta (order 4) with fixed step size $1e^{-06}$. The simulation was carried out in discrete time domain with sampling time interval $1e^{-06}$. The ANN based fundamental source current extraction circuit is implemented using MATLAB level-2 S function with inputs as load current (I_o) and instantaneous phase ($k\omega\Delta\tau$) of source voltage (output of PLL) and outputs as weight W_1^1 and $\sin(k\omega\Delta\tau)$. The code for MATLAB level-2 S function block is as follows:

```
function ANN(block)
setup(block);
function setup(block)

  [1]  % Register the number of ports.

  [2] block.NumInputPorts  =3;
  [3] block.NumOutputPorts = 3;

  [4]  % Set up the port properties to be inherited or dynamic.

  [5] block.SetPreCompInpPortInfoToDynamic;
  [6] block.SetPreCompOutPortInfoToDynamic;

  [7] % Override the input port properties.
  [8] block.InputPort(1).DatatypeID  = 0;  % double
  [9] block.InputPort(1).Complexity  = 'Real';
 [10] block.InputPort(1).Dimensions   = 1;
 [11] block.InputPort(1).SamplingMode = 'Sample';
```

```
[12] block.InputPort(2).DatatypeID  = 0;  % double
[13] block.InputPort(2).Complexity  = 'Real';
[14] block.InputPort(2).Dimensions   = 1;
[15] block.InputPort(2).SamplingMode = 'Sample';
[16] block.InputPort(2).DirectFeedthrough = true;

[17] block.InputPort(3).DatatypeID  = 0;  % double
[18] block.InputPort(3).Complexity  = 'Real';
[19] block.InputPort(3).Dimensions   = 1;
[20] block.InputPort(3).SamplingMode = 'Sample';

[21] % Override the output port properties.

[22] block.OutputPort(1).DatatypeID  = 0; % double
[23] block.OutputPort(1).Complexity  = 'Real';
[24] block.OutputPort(1).Dimensions   = 1;
[25] block.OutputPort(1).SamplingMode = 'Sample';

[26] block.OutputPort(2).DatatypeID  = 0; % double
[27] block.OutputPort(2).Complexity  = 'Real';
[28] block.OutputPort(2).Dimensions   = 1;
[29] block.OutputPort(2).SamplingMode = 'Sample';

[30] block.OutputPort(3).DatatypeID  = 0; % double
[31] block.OutputPort(3).Complexity  = 'Real';
[32] block.OutputPort(3).Dimensions   = 1;
[33] block.OutputPort(3).SamplingMode = 'Sample';

[34] % Register the parameters.

[35] block.NumDialogPrms     = 1;
[36] block.DialogPrmsTunable = {'Tunable'};

[37] block.SetAccelRunOnTLC(true);

[38] block.SimStateCompliance = 'DefaultSimState';

[39] block.RegBlockMethod('CheckParameters', @CheckPrms);
[40] block.RegBlockMethod('PostPropagationSetup', @DoPostPropSetup);
[41] block.RegBlockMethod('Start', @Start);
[42] block.RegBlockMethod('Outputs', @Outputs);

[43] function CheckPrms(block)
[44] mu = block.DialogPrm(1).Data;

[45] if mu <= 0 || mu > 1
[46] error(message('simdemos:neural:stepSize'));
[47] end
```

```
[48] block.AutoUpdateRuntimePrms;

[49] function DoPostPropSetup(block)
[50] block.NumDworks = 1;

[51] block.Dwork(1).Name            = 'w';
[52] block.Dwork(1).Dimensions      = 2;
[53] block.Dwork(1).DatatypeID      = 0;      % double
[54] block.Dwork(1).Complexity      = 'Real'; % real
[55] block.Dwork(1).UsedAsDiscState = true;

[56] % Register all tunable parameters as runtime parameters.

[57] block.AutoRegRuntimePrms;

[58] function Start(block)

[59] block.Dwork(1).Data = [2;1];

[60] function Outputs(block)
[61] mu = block.RuntimePrm(1).Data;
[62] a = block.InputPort(1).Data;
[63] b = block.InputPort(2).data;
[64] e = block.InputPort(3).data;
[65] w =  block.Dwork(1).Data;
[66] x = [a;b];
[67] w = w + (mu*e*x);
[68] block.Dwork(1).Data = w;
[69] block.OutputPort(1).Data = w(1)*a;
[70] block.OutputPort(2).Data = w(2)*b;
[71] block.OutputPort(3).Data = e
```

MATLAB level-2 S function block uses MATLAB code to make Simulink block, which can handle any type of signal generated in a Simulink model during the run time of simulation. The first step to write the code of the block is to define the number of input and output ports followed by their data-type, complexity, and dimension. Then the number of parameters required to be tuned during the runtime of the simulation is mentioned. All the required function to be carried out by the S-function block are registered and defined properly. The number of weight to be updated during the simulation process along with their dimension and complexity to fulfil the

requirement of ANN in the proposed controller is defined in function DoPostPropSetup(block) of S function. Function Start(block) is used to initialize the weights randomly. Eventually in the function Outputs(block), the proposed weight updating algorithm is implemented and the required output to be taken is defined.

The parameters used for simulation are given in Table- 3.2. R_S is the source resistance. Derivative constant k_d is taken with filter coefficient as 1. The cut-off frequency of low pass filter is set as 80Hz. System performance is analyzed on two different load condition, such as: 1) high load (real power and reactive power consumed by non-linear load is 975 watts and -309 watts respectively); 2) low load (real power and reactive power consumed by non-linear load is 663 watts and -183 watts respectively). Fig.3.4 shows the source voltage and load current waveforms under high load conditions when the source is nominal. The Total Harmonic Distortion (THD) of all voltage and current wave forms are measured up to 50th harmonic to validate the theory.

Table 3.2

System parameters used for MATLAB/Simulation in fixed frequency adaptive SM controller

L- 5 mH	V_S^{RMS} - 110 V	λ - 20000
V_{DC} - *200 V*	f_{V_S} - 60 Hz	K_{1P} - 0.24
C- 1100 µF	f_{Switch} -20 kHz	K_i -10
R_S -2Ω	R - 0.7Ω	ρ =0.00002

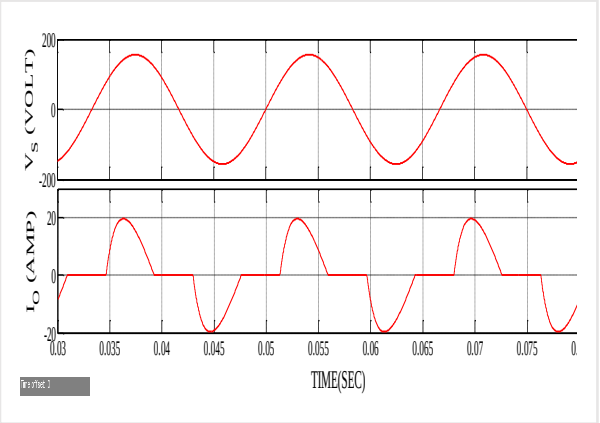

Fig.3.4 Source voltage (top). Load current (bottom). Nominal source. Fixed frequency adaptive SM controller

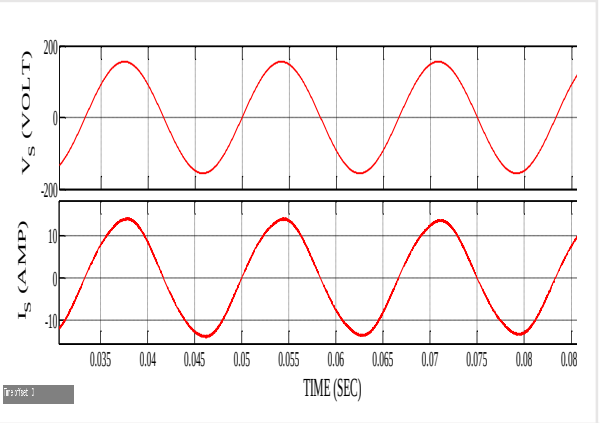

Fig. 3.5 Source voltage (top). Source current (bottom). Nominal source. Fixed frequency adaptive SM controller.

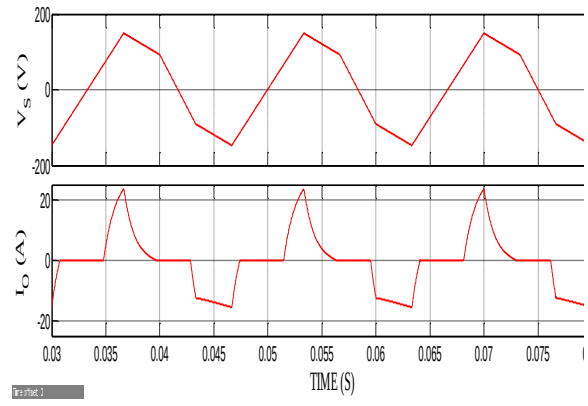

Fig.3.6. Source voltage (top). Load current (bottom). Distorted source. Fixed frequency adaptive SM controller

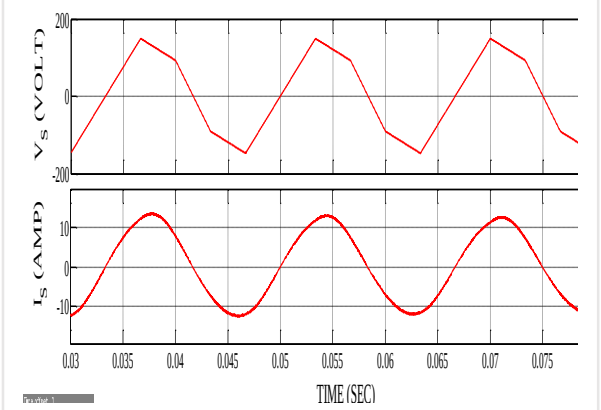

Fig.3.7. Source voltage (top). Source current (bottom). Distorted source. Fixed frequency adaptive SM controller

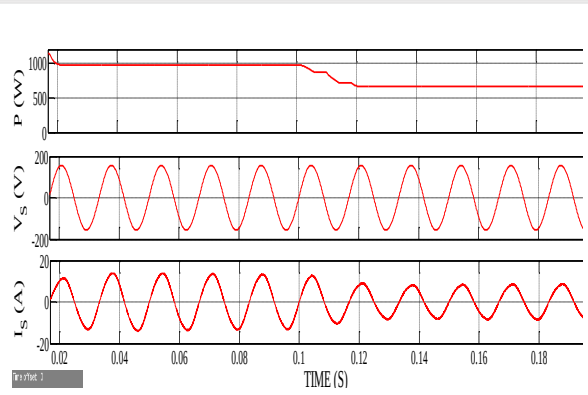

Fig.3.8. Load real power (top). Source voltage (middle). Load current (bottom). High to low nonlinear load. Fixed frequency adaptive SM controller

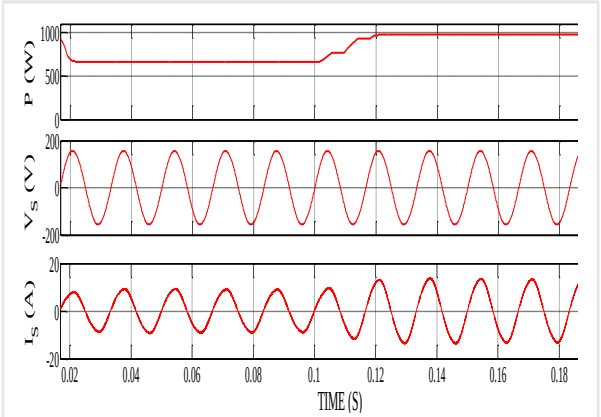

Fig.3.9. Load real power (top). Source voltage (middle), Load current (bottom). Low to high nonlinear load. Fixed frequency adaptive SM controller

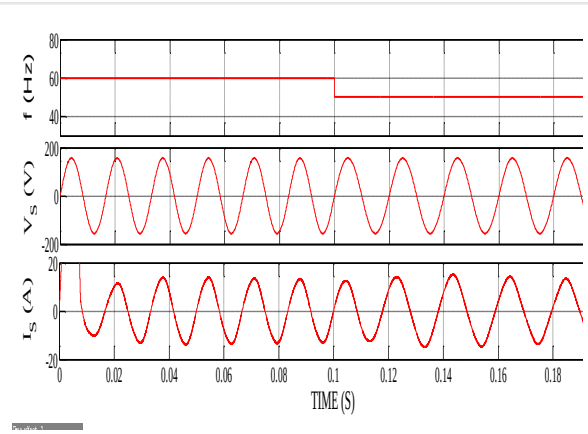

Fig.3.10. Source voltage frequency (top). Source voltage (middle). Source current (bottom). High to low frequency variation. Fixed frequency adaptive SM controller

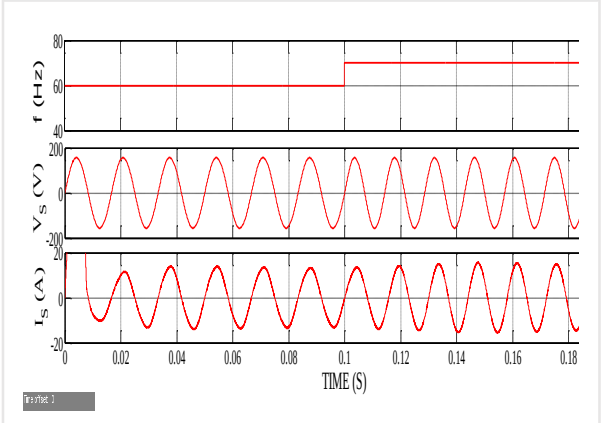

Fig.3.11. Source voltage frequency (top). Source voltage (middle). Source current (bottom). Low to high frequency variation. Fixed frequency adaptive SM controller

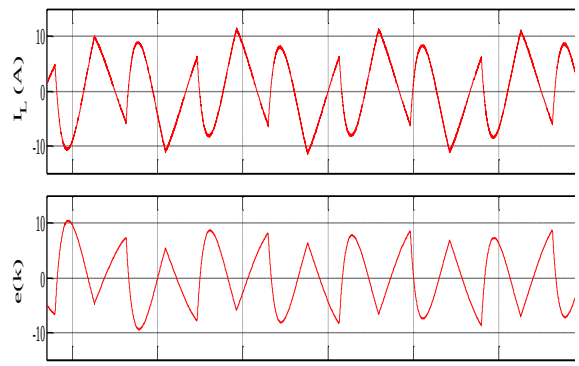

Fig.3.12. Compensating current (top). Error signal (bottom). Nominal source. Fixed frequency adaptive SM controller

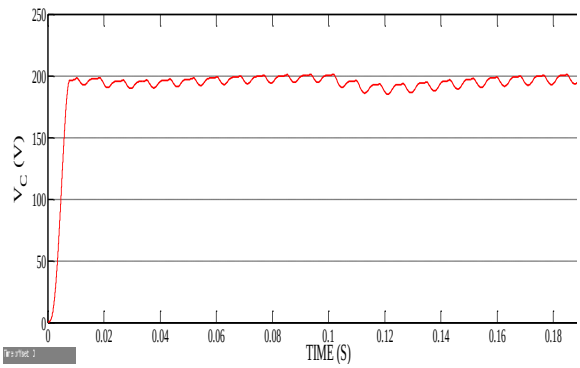

Fig. 3.13. Response of APF capacitor voltage. Nominal source. Fixed frequency adaptive SM controller

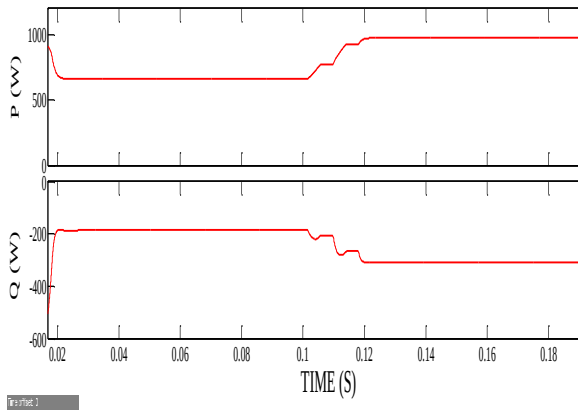

Fig. 3.14. Power consumed by non-linear load. Real power (top). Reactive power (bottom).). Nominal source. Fixed frequency adaptive SM controller

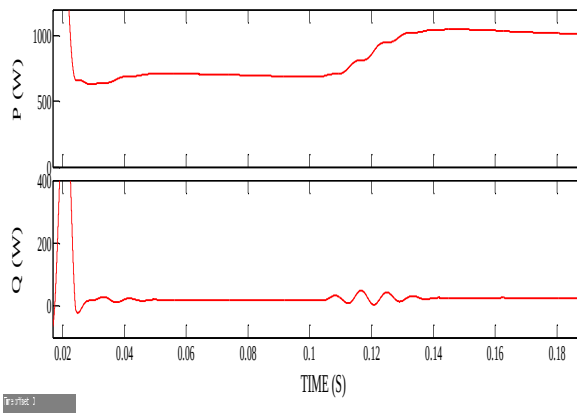

Fig. 3.15. Power delivered by non-linear load. Real power (top). Reactive power (bottom).). Nominal source. Fixed frequency adaptive SM controller

The THD of source voltage and load current is found to be 0% and 52.92 % respectively. Fig. 3.4 shows the waveforms of source voltage and load current. After the application of proposed APF, harmonics are compensated to give the shape of source current same as that of source voltage as shown in Fig. 3.5. THD of the source current is found to be 2.87% measured at time 0.06 second for 2 cycles. In reality voltage source waveforms are found to be distorted. APF proposed in [2] is applicable for both distorted and nominal voltage source, but it is not suitable when frequency of the source voltage is varied more than 2%. The APF proposed in this literature is suitable in wide variation of amplitude and frequency of the source voltage.

Fig.3.6 shows the source voltage and load current waveforms when source is distorted and load is high. Source voltage and load current THD are found to be 7.05% and 59.30% respectively.

After compensation, the source voltage and source current waveforms are shown in Fig.8. THD in the source current is reduced to 2.88% which is very close to the THD in the source current under nominal source and same load conditions. From this it is clear that proposed control strategy is not much affected by source voltage distortion.

Table 3.3

Comparative performance analysis of fixed frequency adaptive SM controller

	THD% High Load and nominal source			THD% Low Load and nominal source			THD% High Load and distorted source			THD% Low Load and distorted source		
	V_S	I_O	I_S	V_S	I_O	I_S	V_S	I_O	I_S	V_S	I_O	I_S
Controller [1]	0.00	52.9	6.22	0.00	68.06	7.22	7.05	59.30	9.44	7.05	76.95	11.23
Controller [2]	0.00	52.9	4.89	0.00	68.06	5.91	7.05	59.30	5.11	7.05	76.95	6.23
Controller [4]	0.00	52.9	3.51	0.00	68.06	4.52	7.05	59.30	7.97	7.05	76.95	8.74
Proposed controller	0.00	52.9	2.87	0.00	68.06	3.59	7.05	59.30	2.88	7.05	76.95	4.31

Fig. 3.8 and Fig.3.9 verifies the adaptive behavior of the proposed control strategy under step load changes. The variation of the source current with high to low nonlinear load variation is shown in Fig.3.8. Similarly source current waveforms for low to high nonlinear load variation is shown in Fig.3.9. From both the Figures it is clear that proposed control strategy gives good transient response and adaptive behavior under step load changes. As shown in table-3.3, there is little variation in source current THD for step load changes. This is because of fixed frequency operation of the proposed APF. Load change causes the change in hysteresis band of the source current under fixed frequency operation.

Fig. 3.10 and Fig. 3.11 show the behavior of the proposed control strategy under wide range of frequency variation. It is clear that proposed APF adopts itself to different frequencies within very short interval of time, so that there is no significant phase difference between source voltage and source current. As shown in Fig. 3.13 the filter capacitor voltage is maintained at desired reference level of 200 V. It is found that there is small deviation from reference filter capacitor voltage at $t = 0.01\text{sec}$ due to the step load changes. Thus, one can tell the transient response of the

proposed controller is quite good. Fig. 3.12 shows the compensating current for compensating the harmonics from the source current and the error signal $e(k)$ which instead of converging to zero converges to a periodic wave.

Active and reactive power consumed by nonlinear load is shown in Fig.3.14. Active and reactive power delivered by source is shown in Fig.3.15. As shown in Fig.3.15 reactive power almost compensated by the proposed control strategy. Performance of the proposed APF is compared with different control strategies presented in [1],[2], and [4] under both nominal and distorted voltage source for different load conditions. Comparative THD analysis is shown in Table 3.3. Proposed APF gives reduced harmonic content in the source current for every source and load conditions.

3.5. Chapter summary

In this chapter a different control strategy for single phase shunt APF for current harmonic elimination is presented. A proper combination of fixed frequency sliding mode current control, ANN based fundamental source current extraction circuit and unipolar PWM increases the dynamic response of APF system with reduced harmonic content in the source current. Fixed frequency SM current control strategy is explained properly. Reference current calculation using ANN and PD controller is explained. Simulation results are analyzed under different load and source conditions. System performance is compared with 3 different control strategies. Hardware implementation of the proposed circuit will be done in the near future.

CHAPTER 4

A PARTIAL FEEDBACK LINEARIZATION BASED APPROACH TO SINGLE PHASE SHUNT ACTIVE POWER FILTER DESIGN

4.1. Introduction

Several control strategies have been proposed in the literature to control the power electronic systems. Among these control strategies, feedback linearization based control of power converters is an effective means to analyze stability of the complete nonlinear system. Thus, the application of feedback linearization to shunt APF control design can be a good choice [3], [30]. As per discussion in chapter 1, relative degree of a system is the determining factor whether the system is partially feedback linearizable or completely feedback linearizable.

The nonlinear system having relative degree lower than the order of the system can be partially linearizeable. However by application of Tellegen's theorem, the system can be exactly linearizable [3]. Single phase shunt APF, DC-DC boost converters are examples of second order system and they have relative degree one [3],[32]. Partial Feedback Linearization (PFL) method has been applied to DC-DC boost converter in [32], whereas Exact Feedback Linearization (EFL) technique has been applied to boost converter in [33]. Due to difficulties in practical implementation of EFL based control of APF system, EFL technique via SM control has been proposed in [3] to control the single phase shunt APF system for improving the performance. In this method authors used an alternating switching scheme to implement the control algorithm. Due to this switching scheme, original property of feedback linearization control technique is lost. Also different output function, can be derived using Tellegen's theorem to control the compensating current in EFL based controller of APF. As shunt APF falls under the category of systems having relative degree one, the straightforward PFL based controller can be applied to shunt APF system. Using PFL based controller in APF, compensating current can be controlled directly by considering it as the output function. Also practical implementation of PFL based controller of APF is easier than the EFL based controller of APF. As discussed before, it is required to ensure

the stability of the internal dynamics of the system in PFL based controller. The dynamics of the system which are not linearized or remains unobservable during feedback linearization are treated as internal dynamics of the system. The averaged dynamic model of shunt APF is used for PFL and internal dynamic stability analysis of APF system. The average model of the active power filter system is obtained by averaging the filter capacitor voltage and coupling inductor current over a complete switching cycle. The usual unipolar pulse width modulation based switching scheme [13] is applied in the proposed PFL based controller of shunt APF. Thus the switching frequency of the APF remains constant. As a result the drawbacks of varying switching frequency can also be overcome with this proposed controller [13].

4.2. Chapter objectives

This chapter exploited PFL technique to control deign of a single phase shunt APF. The nonlinear system dynamics of the APF has been partially feedback linearized using its average dynamic model. New control input to the linearized system is obtained considering the stability of the complete APF system. After that, control input to APF is derived by nonlinear transformation. Stability of the internal dynamics of the system is analyzed considering zero dynamics of the system. This chapter also briefly explains EFL of APF via SM control in which the original property of feedback linearization is lost due to the employed alternative switching scheme. A prototype of the APF system is built and the proposed controller is implemented using dSPACE 1104. Both MATLAB/Simulink based simulation results and experimental results are presented to validate the performance of the controller by comparing it with the controller reported in [3].

4.3. Averaged dynamic model of shunt APF

Structure of a single phase shunt APF, used for analysis of the proposed controller is shown in Fig. 1. A high resistance is connected across the filter capacitor signifies the leakage current flow from positive plate to negative plate of the capacitor throughout the switching cycle. Equivalent circuit of shunt APF for positive inductor current is shown Fig. 2. u is the duty ratio and T is the total switching period. The internal resistance R of the inductor is neglected in the equivalent circuit. Applying Krichoff's voltage law and Krichoff's current law to the equivalent circuit of shunt APF as shown in Fig. 4.2, the state space averaged model of the shunt APF can be written as follows:

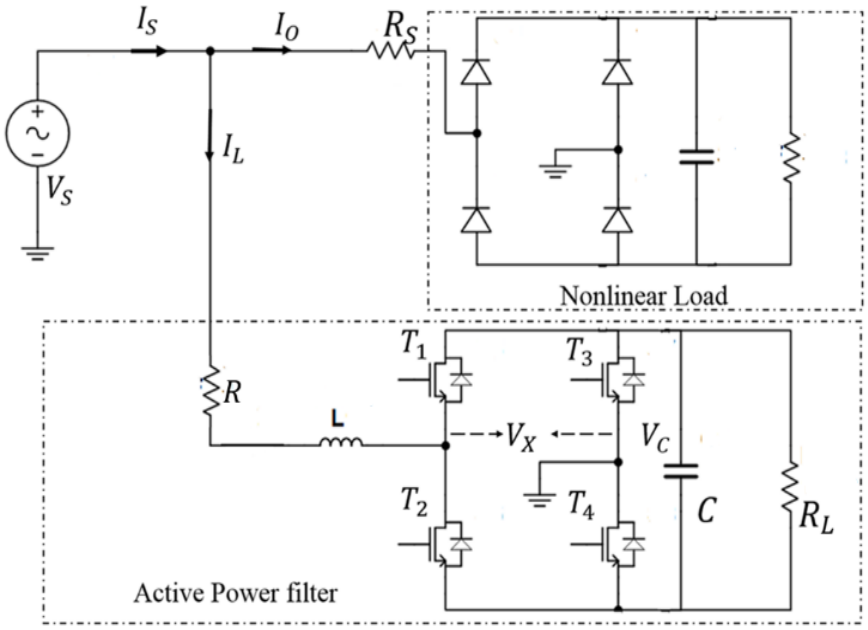

Fig. 4.1. Single phase shunt active power

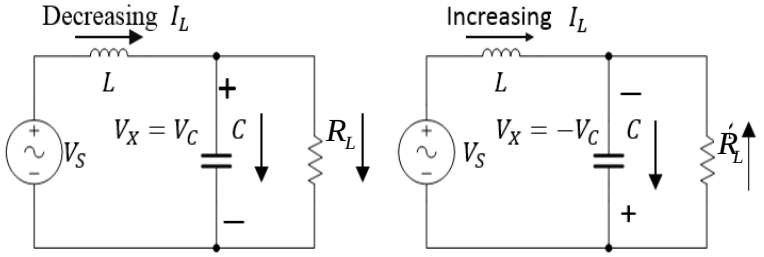

(*a*) (*b*)

Fig. 4.2. Equivalent circuit of active power filter. (a) $0 \le t \le uT$ (b) $uT \le t \le T$

$$L\frac{dx_1}{dt} = (V_S - V_C)u + (V_C + V_S)(1-u) \tag{4.1}$$

$$C\frac{dx_2}{dt} = (I_L - \frac{V_C}{R_L})u + (-\frac{V_C}{R_L} - I_L)(1-u) \tag{4.2}$$

The average values of inductor current and capacitor voltage over a switching cycle are respectively chosen as state variables x_1 and x_2. Thus x_1 and x_2 can be expressed as

$$x_1 = \frac{1}{T}\int_{t}^{t+T} I_L(k)dk \tag{4.3}$$

$$x_2 = \frac{1}{T}\int_{t}^{t+T} V_C(k)dk \tag{4.4}$$

Equations (4.1) and (4.2) can be put to a SISO nonlinear system equation as

$$\dot{X} = f(X) + g(X)u \tag{4.5}$$

where $f(X) = \begin{pmatrix} \frac{x_2}{L} + \frac{V_S}{L} \\ -\frac{x_1}{C} - \frac{x_2}{RC} \end{pmatrix}$, $g(X) = \begin{pmatrix} -\frac{2x_2}{L} \\ \frac{2x_1}{C} \end{pmatrix}$ and $X = [x_1 \; x_2]^T$. Consider the inductor current as the output function is taken as $y = h(x) = x_1$.

4.4. Feedback linearization based controller design for APF

This section presents internal dynamics stability analysis of the APF system and derivation of control input of APF in proposed PFL based controller design considering stability of the complete system. This section also presents EFL of APF via sliding mode control technique, in which the property of feedback linearization is lost due to the employed alternation switching scheme

4.4.1. Partial feedback linearization

Differentiating output function *y* with respect to time one can get

$$\dot{y} = L_f h(x) + L_g h(x)u \tag{4.6}$$

where $L_f h(x)$ and $L_g h(x)$ are Lie derivatives of $h(x)$ with respect to f and g respectively. The relative degree of the system can be obtained by finding the values of $L_f h(x)$ and $L_g h(x)$.

$$L_f h(x) = \frac{\partial h(x)}{\partial x} f(x) = \frac{1}{L}x_2 + \frac{V_S}{L} \tag{4.7}$$

$$L_g h(x) = \frac{\partial h(x)}{\partial x} g(x) = -\frac{2x_2}{L} \tag{4.8}$$

As $L_g h(x) \neq 0$, the second order system has relative degree one [61]. Hence, the system can be partially linearizable. The stability of the internal dynamics must be verified to ensure

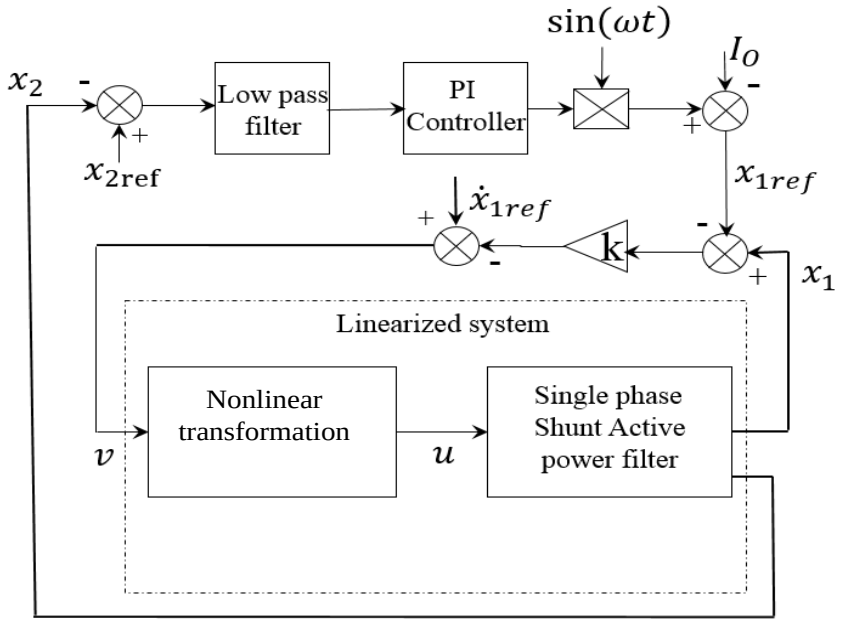

Fig.4.3. Proposed PFL based controller

the stability of the APF system. The internal dynamics of the APF system can be expressed as

$$\dot{\delta} = f(\alpha, \delta) \tag{4.9}$$

where δ is a vector such that $L_g \delta(x) = 0$ and $y = \alpha = x_1$.

One can write

$$L_g \delta(x) = \frac{\partial \delta(x)}{\partial x} g(x) = -\frac{2x_2}{L}\frac{\partial \delta(x)}{\partial x_1} + \frac{2x_1}{C}\frac{\partial \delta(x)}{\partial x_2} = 0 \tag{4.10}$$

One solution of (4.10) is as follows:

$$\delta(x) = \frac{x_1^2}{C} + \frac{x_2^2}{L} \tag{4.11}$$

Differentiating (4.11) with respect to time and using (4.5) one obtains

$$\dot{\delta}(x) = \frac{2V_S}{LC} x_1 - \frac{2x_2^2}{LCR_L} \tag{4.12}$$

As $y = \alpha = x_1$, using (4.11) and (4.12) one can get

$$\dot{\delta}(x) = \frac{2V_S\alpha}{LC} - \frac{2}{CR_L}\{\delta(x) - \frac{\alpha^2}{C}\} \tag{4.13}$$

The stability of the internal dynamics of APF system can be ensured by considering the zero dynamics of the system, which can be obtained by substituting $\alpha = 0$ in (4.13). The zero dynamics of the system is given by

$$\dot{\delta} = -\frac{2\delta}{R_L C} \tag{4.14}$$

There are different solutions of (4.10), but all the solutions lead to an expression similar to that of expression in (4.14). The phase plot of the zero dynamics moves through origin having negative slope as shown in Fig.4.4. This conforms the stability of the internal dynamics of the system.

After analyzing the internal stability of the system, the next step is derive a control input using the proposed PFL based control of shunt APF. By taking the control input u of expression in (4.6) as

$$u = \frac{-L_f h(x) + v}{L_g h(x)} \tag{4.15}$$

the expression for the output can be written as

$$\dot{y} = v \tag{4.16}$$

where v is the new control input to the feedback linearized system in Fig. 4.3. In order to ensure the stability of the complete APF system, the new control input is taken as

$$v = \dot{x}_{1ref} - ke = \dot{x}_{1ref} - k(x_1 - x_{1ref}) = \dot{x}_{1ref} - k(I_S - I_S^*), k > 0 \tag{4.17}$$

x_{1ref} is reference inductor current. Here $'k'$determines the convergent speed of the source current. With positive $'k'$the reference source current will track the actual source current exponentially. The proposed PFL based controller is shown in Fig. 3. The peak value of reference source current is taken as the output of the proportional-integral (PI) controller. It is multiplied with the unit vector of source voltage ($\sin(\omega t)$) to generate the reference source current. x_{2ref} is the reference value of filter capacitor voltage .

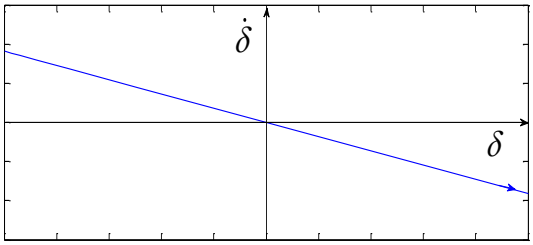

Fig. 4.4. Phase plot of zero dynamics of APF in PFL based controller

4.4.2. Exact feedback linearization

In EFL of APF via SM control a different control output function is chosen to control the compensating current indirectly by the application of Tellegen's theorem. The output function $\hat{y} = \beta(x)$ must satisfy the following condition

$$L_g \beta(x) = \frac{\partial \beta(x)}{\partial x} g(x) = 0 \tag{4.18}$$

From (4.18), one output function can be derived as follows:

$$\hat{y} = \beta(x) = \frac{1}{2} C x_2^2 + \frac{1}{2} L x_1^2 \tag{4.19}$$

With the above output function $\beta(x)$ the system can be transformed to equivalent linear system by nonlinear transformation. After finding $L_f^2 \beta(x)$ and $L_g L_f \beta(x)$, the control input of shunt APF by EFL method can be derived using the control law given below [61]:

$$u = \frac{-L_f^2 \beta(x) + \hat{v}}{L_g L_f \beta(x)} \tag{4.20}$$

$\hat{v}$ is the new control input to the shunt APF. $L_f^2 \beta(x)$ and $L_g L_f \beta(x)$ are Lie derivatives of $L_f \beta(x)$ with respect to f and g respectively. The control law in (4.20) can establish a unique relationship between the output function $\hat{y}$ and new control input as

$$\ddot{\hat{y}} = \hat{v} \tag{4.21}$$

The output function will track the reference output function, if $\hat{v}$ is taken as follows [11]:

$$\hat{v} = \ddot{\hat{y}}_{ref} - k_1 \dot{\hat{e}} - k_2 \hat{e} \tag{4.22}$$

where $\hat{y}_{ref}$ is the reference output function and $\hat{e} = \hat{y} - \hat{y}_{ref}$.

Using the assumption for $\hat{v}$ in (21) we can obtain an expression given below:

$$\ddot{\hat{e}} + k_1\dot{\hat{e}} + k_2\hat{e} = 0 \tag{4.23}$$

The constants k_1 and k_2 are chosen suitably, so that the Routh's characteristic polynomial $s^2 + k_1 s + k_2$ is Hurtwitz.

In [3], in order to avoid calculation and problems related to practical implementation, EFL based control technique is applied to APF via sliding mode control. In this simplified control strategy the expression (4.23) is compared with sliding mode control invariant condition for system trajectory to slide on the sliding surface, which can be stated as follows:

$$\ddot{\hat{e}} + k_1\dot{\hat{e}} + k_2\hat{e} = \dot{S} = 0 \tag{4.24}$$

where S is sliding surface. Using the averaged model of shunt APF as stated in (5) and neglecting R_L as in [3], one can get

$$\frac{d\beta(x)}{dt} = V_S x_1 \tag{4.25}$$

Integration of the above expression leads to

$$\beta(x) = \hat{y} = \int V_S x_1 \tag{4.26}$$

From (4.24) and (4.26) one obtains

$$S = V_S(x_1 - x_{1ref}) + k_1\int V_S(x_1 - x_{1ref}) + k_2\int\int V_S(x_1 - x_{1ref}) \tag{4.27}$$

As $(x_1 - x_{1ref}) = (I_S - I_S^*)$ one can define sliding surface as follows:

$$S = V_S(I_S - I_S^*) + k_1\int V_S(I_S - I_S^*) + k_2\int\int V_S(I_S - I_S^*) \tag{4.28}$$

Controller along with switching scheme used in EFL of APF via sliding mode control is shown in Fig. 5. $V_{DC} = x_{2ref}$ is the reference value of filter capacitor voltage. Two types of switching control schemes are generally being applied to control the switching frequency of APF in sliding mode control strategy. One is unipolar switching scheme and another is bipolar switching scheme.

Unipolar modulation based switching scheme applied in [1] is given in Table 4.1. In this switching scheme, sliding surface is taken as $I_S - I_S^*$. For further analysis, three variables namely R, P and Q are assumed as follows:

$$R = \begin{cases} 1 & \text{if } I_S - I_S^* > 0 \\ 0 & \text{if } I_S - I_S^* < 0 \end{cases}, Q = \begin{cases} 1 & \text{if } V_S > 0 \\ 0 & \text{if } V_S < 0 \end{cases}, \quad P = \begin{cases} 1 & \text{if } (I_S - I_S^*)V_S > 0 \\ 0 & \text{if } (I_S - I_S^*)V_S < 0 \end{cases}$$

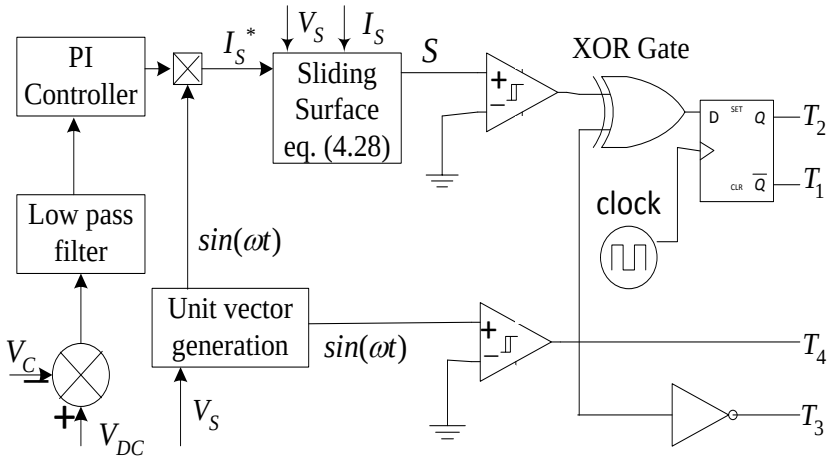

Fig. 4.5. Controller implemented in [3]

Table 4.1

Switching scheme used in [1]

	$V_S > 0$	$V_S < 0$		$I_S - I_S^* > 0$	$I_S - I_S^* < 0$
T_3	0	1	T_1	1	0
T_4	1	0	T_2	0	1

Table 4.2

Switching scheme used in [3]

	$V_S > 0$	$V_S < 0$		$S > 0$	$S < 0$
T_3	0	1	T_1	$0 \oplus Q$	$1 \oplus Q$
T_4	1	0	T_2	$1 \oplus Q$	$0 \oplus Q$

The alternate unipolar switching scheme used in EFL of APF via sliding mode control is given in Table 4.2. As shown in Fig. 4.5 an XOR gate is used in the switching scheme employed in [3]. In the Table 4.3, the concept behind the use of XOR gate is explained. In Table 4.3, when $V_S > 0$ and $I_S - I_S^* > 0$, $V_S(I_S - I_S^*) > 0$ and Q, R, P take their corresponding assumed values. Similarly Q, R, P values for all possible conditions are given in Table 4.3. Observing all the columns of Table 4.3, one can easily verify that $R = P \odot Q = \overline{P \oplus Q}$. The multiplication of V_S with $(I_S - I_S^*)$ becomes meaningless by use of XNOR gate. As inverting pulses are given to the switches of one leg of an APF, XNOR gate can be replaced by XOR gate by feeding inverting pulses to switches T_1 and T_2. As shown in Table 4.2, similar switching scheme is applied in [3].

Table 4.3

$V_S > 0, Q = 1$	$I_S - I_S^* > 0, R = 1$	$V_S(I_S - I_S^*) > 0, P = 1$
$V_S > 0, Q = 1$	$I_S - I_S^* < 0, R = 0$	$V_S(I_S - I_S^*) < 0, P = 0$
$V_S < 0, Q = 0$	$I_S - I_S^* > 0, R = 1$	$V_S(I_S - I_S^*) < 0, P = 0$
$V_S < 0, Q = 0$	$I_S - I_S^* < 0, R = 0$	$V_S(I_S - I_S^*) > 0, P = 1$

Thus, with this alternate explained switched scheme the sliding surface $V_S(I_S - I_S^*)$ is same as that of sliding surface $(I_S - I_S^*)$. Similarly the sliding surface in (4.28) is same as that of sliding surface given below:

$$S = (I_S - I_S^*) + k_1 \int (I_S - I_S^*) + k_2 \int\int (I_S - I_S^*) \tag{4.29}$$

This implies the output function, $\beta(x) = \int V_S x_1$ derived using Tellegen's theorem in EFL of APF via sliding mode control is not taking part in the sliding surface design . Thus, the property of feedback linearization is almost lost in this control strategy.

4.5. Results and discussions

4.5.1. Simulation results

In this section performance of EFL of APF via sliding mode control proposed in [3] is compared with performance of PFLbased controller proposed in this chapter. Simulations are carried out in discrete time domain using MATLAB/Simulink. The solver chosen as Dormand-

Prince (ode45) in variable step with discrete time interval $5e^{-06}$. Reference current is being generated in both PFL and EFL techniques by using a PI controller. Cut off frequency of low pass filter, used in both the techniques before PI controller to reduce harmonic content in source current is taken as 80Hz. The parameters used for simulation are given in Table 4.4. THD is measured up to 50th harmonics at 0.3 second for 2 cycles to verify the performance of both the techniques.

Table 4.4

System parameters used for Simulation for comparative analysis of both PFL and EFL based controller

L- 5 mH	V_S^{RMS} - 110 V	$k = 10000$
V_{DC} - *200 V*	f_{V_S} - 60 Hz	$k_P = .25$
C- 1100 µF	$k_1 = 4500$	K_i -10
f_{Switch} -20 kHz	$k_2 = 15000$	$R_L = 10k\Omega$

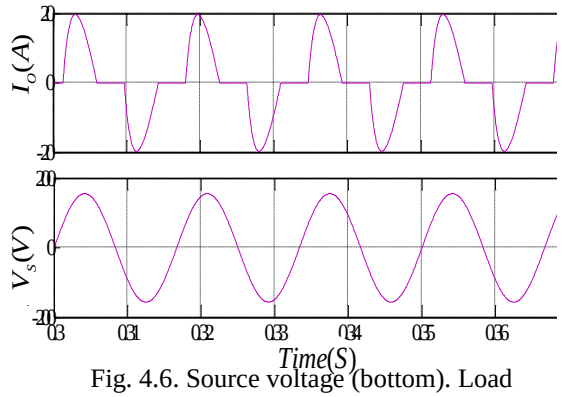

Fig. 4.6. Source voltage (bottom). Load current (top). PFL based controller

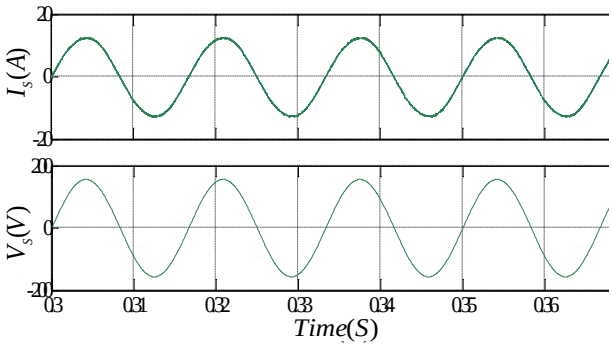

Fig. 4.7. Source voltage (bottom). Source current (top). PFL based controller

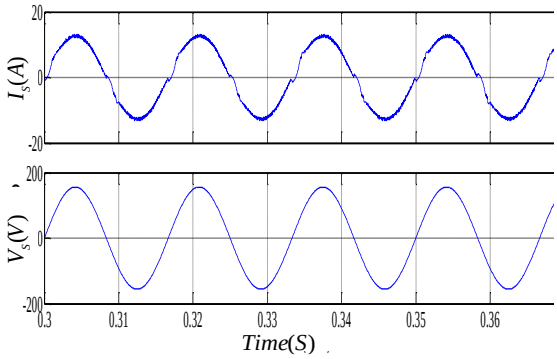

Fig. 4.8. Source voltage (bottom). Source current (top). Controller reported in [3]

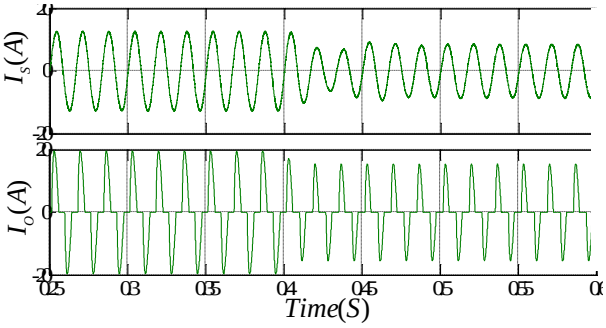

Fig.4. 9. Response for load change. Load current (bottom). Source current (top). PFL based controller

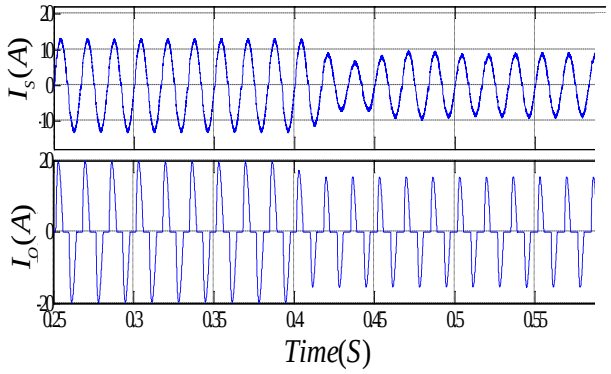

Fig. 4.10. Response for load change. Load current (bottom). Source current (top). Controller reported in

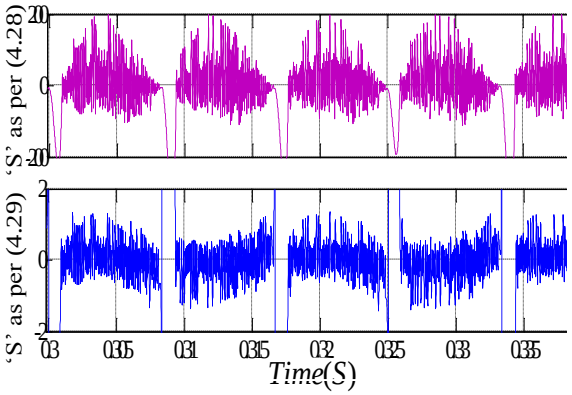

Fig.4.11. Tracking of sliding surface trajectory, 'S' as per (4.28) top, 'S' as per (4.29) bottom. Controller reported in [3]

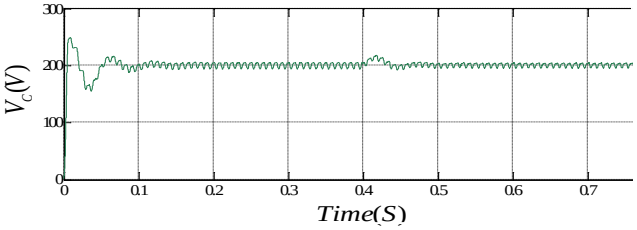

Fig. 4.12. Filter capacitor voltage. PFL based controller.

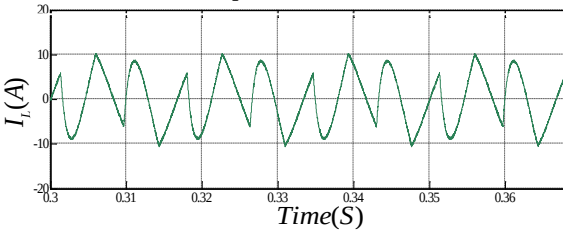

Fig. 4.13. Inductor current. PFL based controller

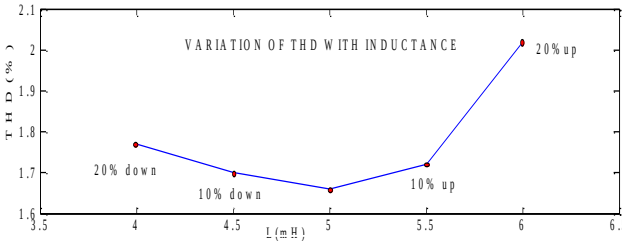

Fig. 4.14. Variation of THD with parameter inductance. PFL based controller

Maximum switching frequency (f_s) is taken constant for both PFL and EFL techniques. k_p and k_i are proportional and integral gains of the PI controller. THDs of load current and source voltage are found to be 52.93% and 0% respectively. The waveforms of source voltage and load current are shown in Fig. 4.6. With the PFL based controller source current THD has been reduced to 1.63% (shown in Fig. 4.7). Further it can be seen that source current is found to be in same phase to that of source voltage, whereas source current THD in EFL of APF via sliding mode control is 5.12%. The wave forms of source voltage and source current for EFL via sliding mode controller are shown in Fig. 4.8.

To compare the transient responses of both the controllers, simulations are carried out for a sudden load change from 100% to 75% of full load at 0.4 sec. From Fig. 4.9 and Fig.4.10, it is

clear that there is no significant difference is observed between the transient responses of PFL based controller and EFL via sliding mode controller as transient response mostly depends on how the reference source current is generated. The filter capacitor voltage is maintained approximately at a constant value of 200V in PFL based controller as shown in Fig. 4.12. The inductor current or the compensating current required to compensate the harmonics from source current is shown in Fig.4.13. This inductor current is equal to the sum of the harmonic components of load current but with opposite polarity.

Performance of the proposed PFL based controller is tested under coupling inductance variation. As shown in Fig. 4.14, there is not much difference in THD for 20% up/down variation of inductance. Thus, the proposed controller is robust against inductance variations.

Fig. 4.11 shows the variation of sliding surface trajectory 'S'with respect to the surface $S=0$. It is found that there is larger variation of sliding surface (Fig. 4.11, top) as defined in eq. (4.28) than the surface (Fig. 4.11, bottom) as defined in eq. (4.29). Sliding in the vicinity of the sliding surface $S=0$ occurs by the sliding surface as stated in (30). This implies that the output function $\beta(x)$ has no role in the design of the sliding surface. This conforms the loss of property of feedback linearization in [3].

4.5.2. Experimental results

In this section selected experimental results are provided to verify the performance of the proposed controller. The block diagram of complete hardware structure is shown in Fig. 4.15. The prototype of experimental setup is shown in Fig. 4.16. A bridge rectifier (SQL100A1600V) with a $470\mu F$ electrolytic capacitor and a rheostat are used as a nonlinear load. An auto transformer is used to vary the input source voltage. A SEMIKRON make inverter is connected in parallel in between source and load at the point of common coupling through a ferrite core inductor having inductance 5mH. Out of three legs of the three phase inverter, only two legs have been used in this experiment. The SEMIKRON inverter comprises of dual Insulated Gate Bipolar Transistor (IGBT) drivers (SKHI 22 AR), IGBT switches (SKM 75 GB 123 D) and filter capacitor of capacitance $1100\mu F$ .Two voltage sensors LV 25-P are used for sensing the source voltage and filter capacitor voltage. Two current sensors LA 55-P are used for sensing the desired currents. Sensor circuits are made as per datasheet specifications. The output of the sensors are fed to the dSPACE 1104 control

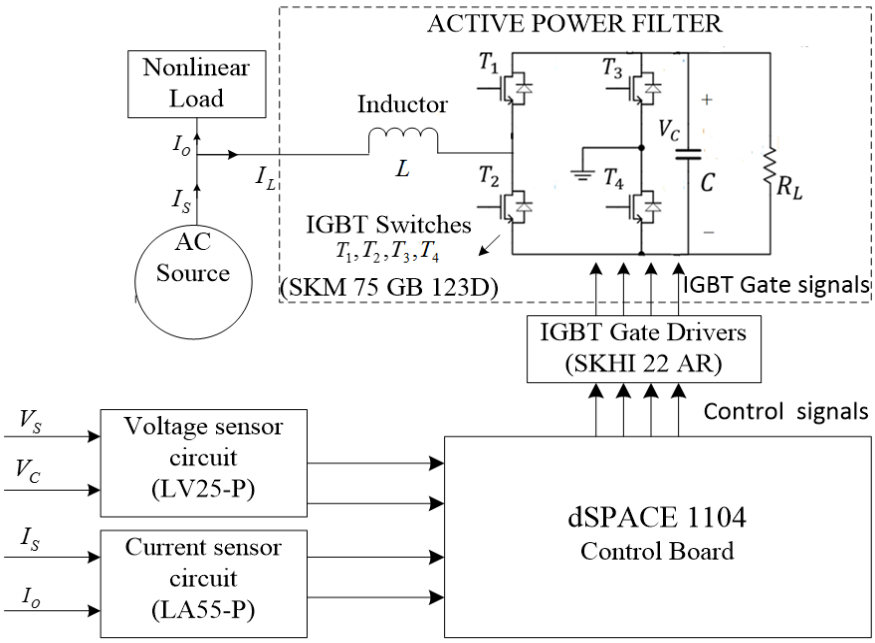

Fig. 4.15. Block diagram of Hardware structure

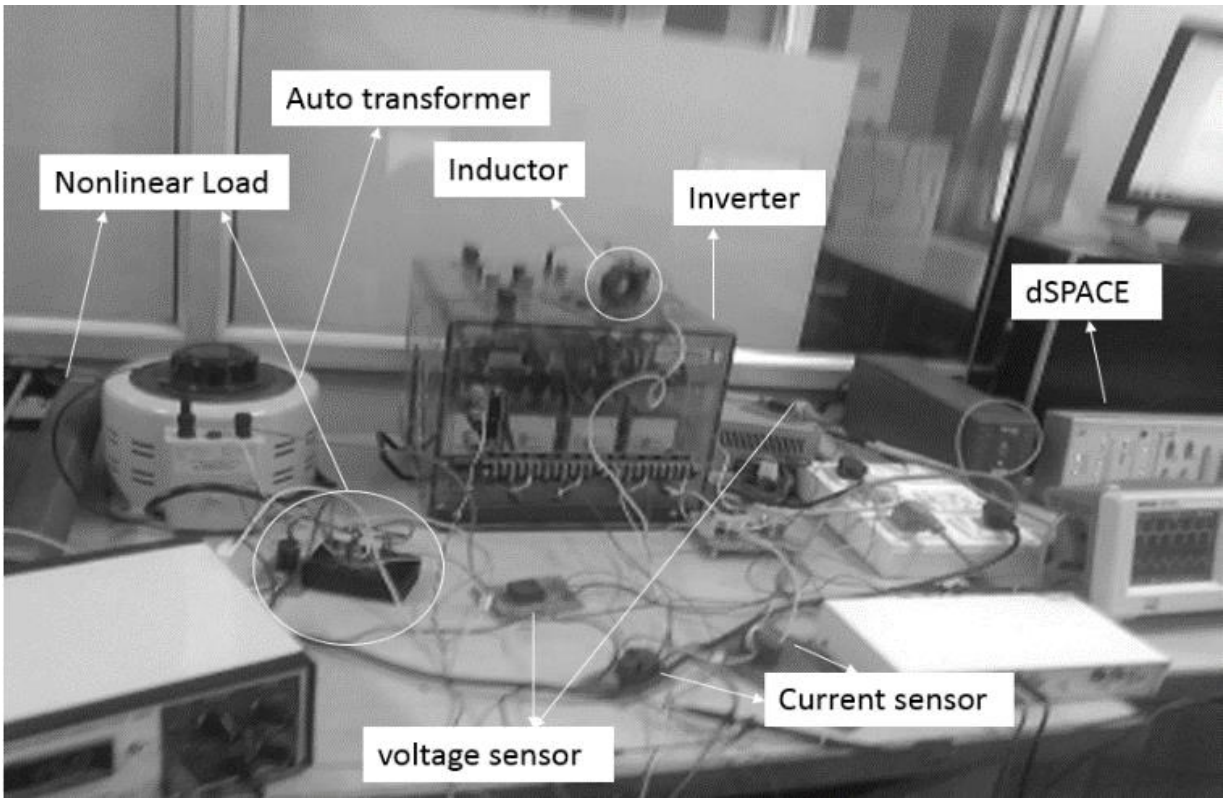

Fig. 4.16. The prototype of the experimental setup

board through analog to digital converter port. The proposed PFL based controller and the controller reported in [6] are implemented using this dSPACE 1104 control board. The required controlled pulses are fed to the IGBT driver input through digital to analog converter port of dSPACE with proper amplification. Waveforms are taken by oscilloscope through digital to analog converter port of dSPACE to avoid noises.

The source voltage and load current waveforms obtained from experimental studies are shown in Fig.4.17. THD of load current is calculated as 73.2%. After implementing the proposed PFL based controller, source voltage and source current waveforms are shown in Fig.4.18. It is found that source is approximately sinusoidal and in same phase to that of source voltage. THD of the source current is found to be 3.96%, which implies the proposed control strategy is exhibiting improved performance.

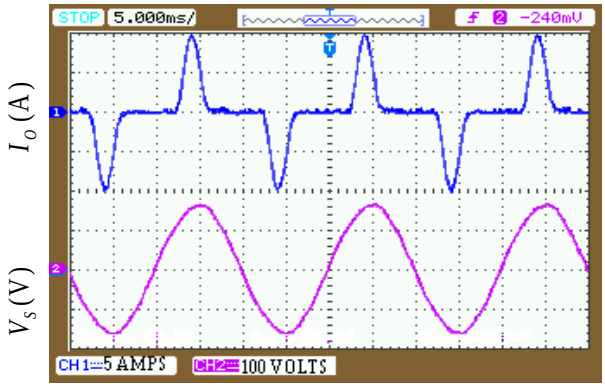

Fig. 4.17. Source voltage (bottom). Load current (top). Experimental results

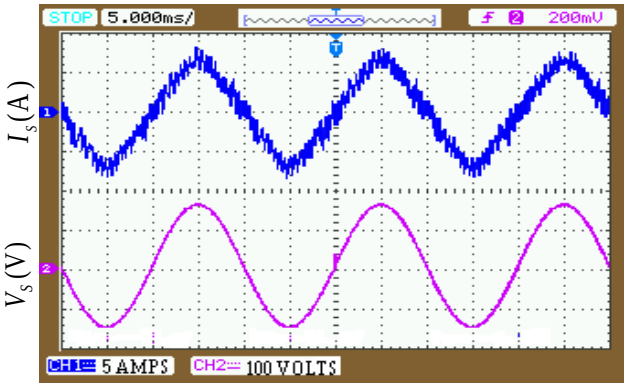

Fig. 4.18. Source voltage (bottom). Source current (top). Experimental results. PFL based controller

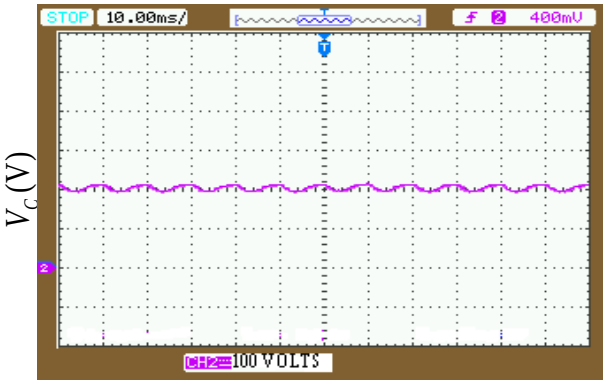

Fig. 4.19. Filter capacitor voltage. Experimental results PFL based controller.

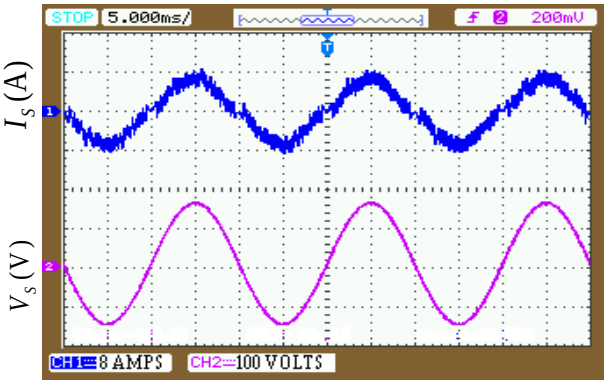

Fig. 4.20. Source voltage (bottom). Source current (top). Experimental results. Controller reported in [3]

Fig.4.19 shows the maintenance of the filter capacitor voltage at desired level of 200 volts in PFL based controller. This is because the reference capacitor voltage in the design of the controller is taken as 200 volts. Source voltage and source current waveforms obtained from experimental studies using the controller reported in [3], are shown in Fig. 4.20. THD of source current in this controller is found to be 6.33%. Thus it is clear that PFL based controller is more suitable than EFL based sliding mode controller for designing APF.

4.6. Chapter summary

In this chapter, a PFL based controller design of shunt APF is reported in which its averaged dynamic model is used. Stability of internal dynamics of APF system in PFL based controller is analyzed. Usual unipolar pulse width modulation based switching scheme is employed for implementation of the proposed control algorithm in both simulation and experimental studies. Analysis of alternate switching scheme of EFL via sliding mode control has been carried out. It is found that with this alternate switching scheme, the property of feedback linearization is almost lost in EFL of APF via sliding mode control. Finally both MATLAB/Simulink and experimental results are provided to compare the results of proposed controller with the controller reported in [3]. It is found that PFL based controller is a better choice because it provides complete stability of the APF system and reduces the source current THD.

CHAPTER 5

A PARTIAL FEEDBACK LINEARIZATION BASED CONTROL DESIGN AND SIMULATION FOR THREE PHASE SHUNT ACTIVE POWER FILTER

5.1. Introduction

As discussed before, a three phase shunt APF is required to eliminate the current harmonics in industry applications. In three phase systems such as three phase UPS inverter [35] and three phase grid connected photo voltaic system [59], PFL based control technique has been applied to improve their performance. Authors of [35] applied PFL based control technique by considering the system as both single input single output (SISO) and multiple input multiple output (MIMO) system. Similarly authors of [60] considered grid connected photovoltaic system as MIMO system for applying PFL based control technique.

Unlike single phase shunt APF, a three phase shunt APF can be considered as a MIMO system. Compensating currents of three phases can be assumed as three outputs of the system for implementing the PFL based control method. A typical structure of three phase APF is shown in Fig.1.5. But for making the system analysis using PFL based control technique easier, a little modification has been carried out in the basic structure of three phase shunt APF. As discussed in chapter 4, a high resistance, connected across the filter capacitor signifies the leakage current flow from positive plate to negative plate of the capacitor throughout the switching cycle. The configuration of three phase shunt APF, taken for consideration in this chapter is shown in Fig. 5.1.

5.2. Chapter objectives

This chapter exploited partial feedback linearization technique to design control of a three phase shunt active power filter (APF) by considering it as a MIMO system. The averaged dynamic model of the three phase APF is derived considering the single phase equivalent circuit of the

system. This averaged dynamic model is used to partially feedback linearize the MIMO nonlinear system dynamics. New control input to the linearized system is obtained considering the stability of the complete APF system. After that, control input to APF is derived by nonlinear transformation. Stability of the internal dynamics of the system is analyzed considering zero dynamics of the system. MATLAB/Simulink based simulation results are provided to validate the performance of the controller.

5.3. Averaged dynamic model of three phase shunt APF

Fig.5.2 shows the equivalent circuit for phase 1 of three phase APF. Similar equivalent circuits can also be obtained for other two phases. I_{L_1} is the compensating current in phase 1. Similarly I_{L_2} and I_{L_3} are taken as the compensating currents of phase 2 and 3 respectively. For analysis V_1, V_2 and V_3 are assumed as the phase to neutral voltages of phase 1, 2 and 3 respectively. The averaged dynamic model of three phase APF can be obtained by averaging the inductor currents and capacitor voltage over a complete switching cycle. Consider u_1, u_2 and u_3 are the duty ratios or the control inputs to legs of APF which are coupled to phase 1,2 and 3 respectively through coupling inductor and T is the total switching period, which remain constant for all legs of APF.

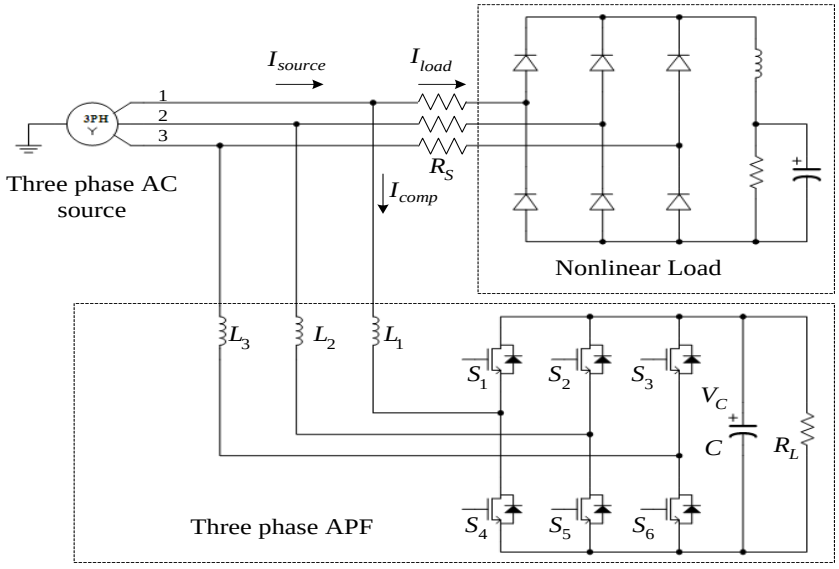

Fig. 5.1. Three phase shunt active power filter

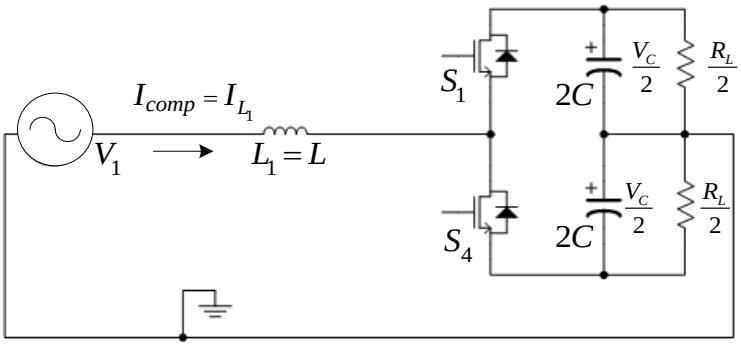

Fig. 5.2. Equivalent circuit for phase 1 of three phase active power filter.

The coupling inductance value for all three phases is kept same for making the analysis easier. So one can write $L_1 = L_2 = L_3 = L$. Considering the equivalent circuit of all three phases and proceeding as in chapter 4, one can get the averaged dynamic model of three phase shunt APF as follows:

$$L\frac{dx_{11}}{dt} = (V_1 - \frac{V_C}{2})u_1 + (V_1 + \frac{V_C}{2})(1-u_1) \tag{5.1}$$

$$L\frac{dx_{12}}{dt} = (V_2 - \frac{V_C}{2})u_2 + (V_2 + \frac{V_C}{2})(1-u_2) \tag{5.2}$$

$$L\frac{dx_{13}}{dt} = (V_3 - \frac{V_C}{2})u_3 + (V_3 + \frac{V_C}{2})(1-u_3) \tag{5.3}$$

$$\begin{aligned} C\frac{dx_{14}}{dt} = \frac{1}{2}\Big\{ &(I_{L_1} - \frac{V_C}{2R_L})u_1 + (I_{L_2} - \frac{V_C}{2R_L})u_1 + (I_{L_3} - \frac{V_C}{2R_L})u_1 + \\ &(-\frac{V_C}{2R_L} - I_{L_1})(1-u_1) + (-\frac{V_C}{2R_L} - I_{L_2})(1-u_2) + (-\frac{V_C}{2R_L} - I_{L_3})(1-u_3)\Big\} \end{aligned} \tag{5.4}$$

The average values of compensating currents for phase 1,2,3 and capacitor voltage over a switching cycle are respectively chosen as state variables x_{11}, x_{12}, x_{13} and x_{14}. Thus, x_{11}, x_{12}, x_{13} and x_{14} can be expressed as

$$x_{11} = \frac{1}{T}\int_{t}^{t+T} I_{L_1}(k)dk \tag{5.5}$$

$$x_{12} = \frac{1}{T}\int_{t}^{t+T} I_{L_2}(k)dk \tag{5.6}$$

$$x_{13} = \frac{1}{T}\int_{t}^{t+T} I_{L_3}(k)dk \tag{5.7}$$

$$x_{14} = \frac{1}{T}\int_{t}^{t+T} V_C(k)dk \tag{5.8}$$

Rearranging (5.1), (5.2), (5.3) and (5.4), one can get the expressions as follows:

$$\frac{dx_{11}}{dt} = \frac{V_1}{L} + \frac{x_{14}}{2L}(1-2u_1) \tag{5.9}$$

$$\frac{dx_{12}}{dt} = \frac{V_2}{L} + \frac{x_{14}}{2L}(1-2u_2) \tag{5.10}$$

$$\frac{dx_{13}}{dt} = \frac{V_3}{L} + \frac{x_{14}}{2L}(1-2u_3) \tag{5.11}$$

$$\frac{dx_{14}}{dt} = \frac{x_{11}}{2C}(2u_1-1) + \frac{x_{12}}{2C}(2u_2-1) + \frac{x_{13}}{2C}(2u_3-1) - \frac{3x_{14}}{4R_LC} \tag{5.12}$$

Equations (5.9), (5.10), (5.11) and (5.12) can be put to a MIMO nonlinear system equation as

$$\dot{X} = f(X) + g_1(X)u_1 + g_2(X)u_2 + g_3(X)u_3 \tag{5.13}$$

where $f(X) = \begin{pmatrix} \frac{x_{14}}{2L} + \frac{V_1}{L} \\ \frac{x_{14}}{2L} + \frac{V_2}{L} \\ \frac{x_{14}}{2L} + \frac{V_3}{L} \\ -\frac{x_{11}}{2C} - \frac{x_{12}}{2C} - \frac{x_{13}}{2C} - \frac{3x_{14}}{4R_LC} \end{pmatrix}$, $g(X) = \begin{pmatrix} -\frac{x_{14}}{L} & 0 & 0 \\ 0 & -\frac{x_{14}}{L} & 0 \\ 0 & 0 & -\frac{x_{14}}{L} \\ -\frac{x_{11}}{C} & -\frac{x_{12}}{C} & -\frac{x_{13}}{C} \end{pmatrix}$ and

$X = [x_{11}\ x_{12}\ x_{13}\ x_{14}]^T$. Consider the compensating currents of three phases as the output functions. Thus, the output functions are as follows:

$$y_1 = h_1(x) = x_{11}. \tag{5.14}$$

$$y_2 = h_2(x) = x_{12} \tag{5.15}$$

$$y_3 = h_3(x) = x_{13} \tag{5.16}$$

5.4. PFL based controller design for three phase APF

The first step in designing the controller of a system using feedback linearization technique is to find the relative degree of the system. For a MIMO system, relative degree should be found out separately for each output function of the system. Total relative degree of the system is the sum of the relative degrees associated with every output functions of the system. Consider r_1, r_2 and r_3 are the relative degrees associated with outputs y_1, y_2 and y_3 respectively. Differentiating output function y_1 with respect to time one can get

$$\dot{y}_1 = L_f h_1(x) + L_{g_1} h_1(x) u_1 \tag{5.17}$$

where $L_f h_1(x)$ and $L_{g_1} h_1(x)$ are Lie derivatives of $h_1(x)$ with respect to f and g_1 respectively. The relative degree of the system can be obtained by finding the values of $L_f h_1(x)$ and $L_{g_1} h_1(x)$.

$$L_f h_1(x) = \frac{\partial h_1(x)}{\partial x} f(x) = \frac{1}{2L} x_{14} + \frac{V_1}{L} \tag{5.18}$$

$$L_{g_1} h_1(x) = \frac{\partial h_1(x)}{\partial x} g_1(x) = -\frac{x_{14}}{L} \tag{5.19}$$

As $L_{g_1} h_1(x) \neq 0$, the relative degree r_1 =1 [61]. Similar procedure can be followed to find the relative degrees r_2 and r_3. It is found that $r_2 = r_3$ =1. Thus, the total relative degree of the MIMO system is $r = r_1 + r_2 + r_3 = 3$. The total order of the system $n = 4$. As $r < n$, the system can be partially linearizable. The stability of the internal dynamics must be verified to ensure the stability of the three phase APF system. The internal dynamics of the three phase APF system can be expressed as

$$\dot{\varphi} = f(y_1, y_2, y_3, \varphi) \tag{5.20}$$

Where φ is a vector such that $L_{g_1}\varphi(x) = L_{g_2}\varphi(x) = L_{g_3}\varphi(x) = 0$

The above condition will be satisfied if

$$\varphi(x) = \frac{1}{2}\left\{ L x_{11}^2 + L x_{12}^2 + L x_{13}^2 + C x_{14}^2 \right\} \tag{5.21}$$

Differentiating (5.21) with respect to time and using (5.13) one obtains

$$\dot{\varphi}(x) = V_1 x_{11} + V_2 x_{12} + V_3 x_{13} - \frac{3x_{14}^2}{4R_L C} \tag{5.22}$$

As $y_1 = x_{11}$, $y_2 = x_{12}$ and $y_3 = x_{13}$ using (5.21) and (5.22) one can get

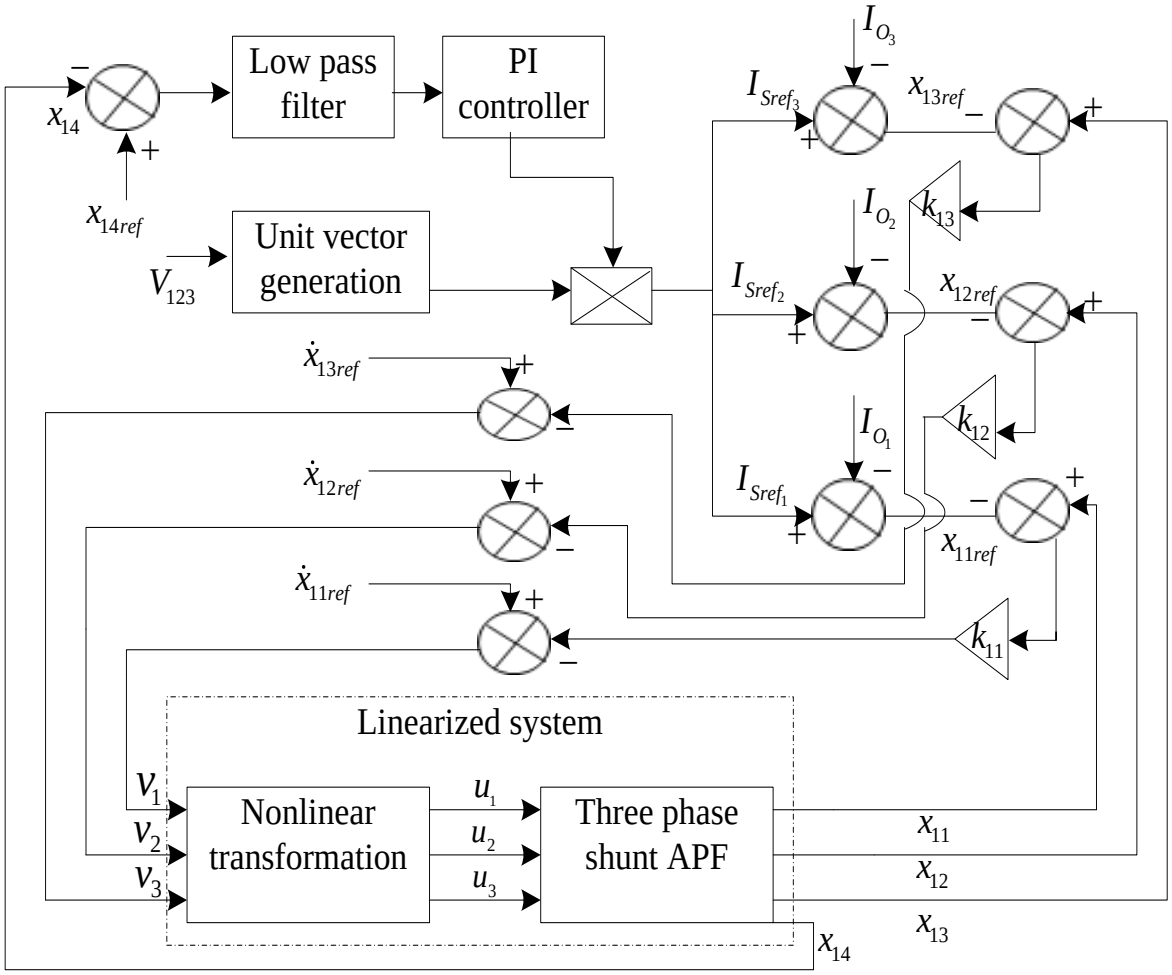

Fig.5.3. PFL based controller for three phase APF

$$\dot{\varphi} = V_1 y_1 + V_2 y_2 + V_3 y_3 - \frac{3}{2R_L C^2}\left(\varphi - \frac{1}{2}Ly_1^2 - \frac{1}{2}Ly_2^2 - \frac{1}{2}Ly_3^2\right) \tag{5.23}$$

The stability of the internal dynamics of APF system can be ensured by considering the zero dynamics of the system. As per discussion in chapter 1, zero dynamics of the system can be

obtained by substituting $y_1 = y_2 = y_3 = 0$ in (5.23). Thus, the zero dynamics of the system is given by

$$\dot{\varphi} = -\frac{3}{2R_L C^2}\varphi \tag{5.24}$$

The phase plot of the zero dynamics will move through origin having negative slope. This conforms the stability of the internal dynamics of the system. After analyzing the internal dynamics stability of the system, the next step is to derive a control input using the proposed PFL based control of three phase shunt APF. By taking the control input u_1 of expression in (5.17) as

$$u_1 = \frac{-L_f h_1(x) + v_1}{L_{g_1} h_1(x)} \tag{5.25}$$

the expression for the output of phase 1 can be written as

$$\dot{y}_1 = v_1 \tag{5.26}$$

where v_1 is the new control input of the feedback linearized system corresponding to output y_1. In order to ensure the stability of the complete APF system, the new control input is taken as

$$v_1 = \dot{x}_{11ref} - ke = \dot{x}_{11ref} - k_{11}(x_{11} - x_{11ref}), k_{11} > 0 \tag{5.27}$$

x_{11ref} is reference compensating current for phase 1. As explained earlier, 'k_{11}' determines the convergent speed of the compensating current. With positive 'k_{11}' the actual compensating current will track the reference compensating current exponentially. Similarly considering the stability of the whole system the new control inputs v_2 and v_3 of the linearized system corresponding to outputs y_2 and y_3 respectively are assumed as follows:

$$v_2 = \dot{x}_{12ref} - ke = \dot{x}_{12ref} - k_{12}(x_{12} - x_{12ref}), k_{12} > 0 \tag{5.28}$$

$$v_3 = \dot{x}_{13ref} - ke = \dot{x}_{13ref} - k_{13}(x_{13} - x_{13ref}), k_{13} > 0 \tag{5.29}$$

x_{12ref} and x_{13ref} are the reference compensating currents of phase 2 and 3 respectively. After that, the original control inputs u_2 and u_3 of the three phase APF system can be found out by nonlinear transformation as follows:

$$u_2 = \frac{-L_f h_2(x) + v_2}{L_{g_2} h_2(x)} \tag{5.30}$$

$$u_3 = \frac{-L_f h_3(x) + v_3}{L_{g_3} h_3(x)} \tag{5.31}$$

The proposed PFL based controller for three phase APF is shown in Fig. 5.3. Reference source currents for all three phases are generated by using PI controller (see Fig.5.3) as in [38]. I_{Sref_1}, I_{Sref_2} and I_{Sref_3} are reference source current of phase 1. 2 and 3 respectively. After that reference compensating currents for all three phases are calculated by subtracting load currents from corresponding reference source currents. I_{O_1}, I_{O_2} and I_{O_3} are the load currents of phase 1, 2 and 3 respectively. x_{14ref} is reference capacitor voltage.

5.5. Results and discussions

In this section simulation results are reported to validate the performance of PFL based controller for three phase APF. Simulations are carried out in discrete time domain using MATLAB/Simulink. The solver chosen as Dormand-Prince (ode45) in variable step with discrete time interval $5e^{-06}$. Cut off frequency of low pass filter, used in this techniques before PI controller to reduce harmonic content in source current is taken as 80Hz. The parameters used for simulation are given in Table 5.1. THD is measured up to 50th harmonics at 0.06 second for 2 cycles to verify the performance of the proposed technique.

Table 5.1

System parameters used for Simulation in PFL based controller for three phase APF

L- 8mH	V_S^{RMS} - 110 V	K_i -10
V_{DC} - *500 V*	f_{V_S} - 50 Hz	$R_L = 10k\Omega$
C- 1100 µF	$k_1 = 10000$	
f_{Switch} -20 kHz	$k_P = .25$	

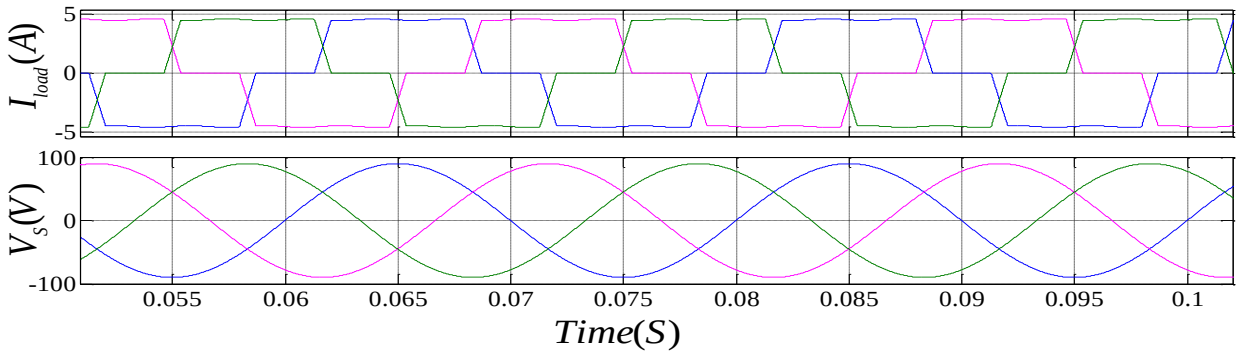

Fig. 5.4. Source voltage (bottom). Load current (top). PFL based controller for three phase APF

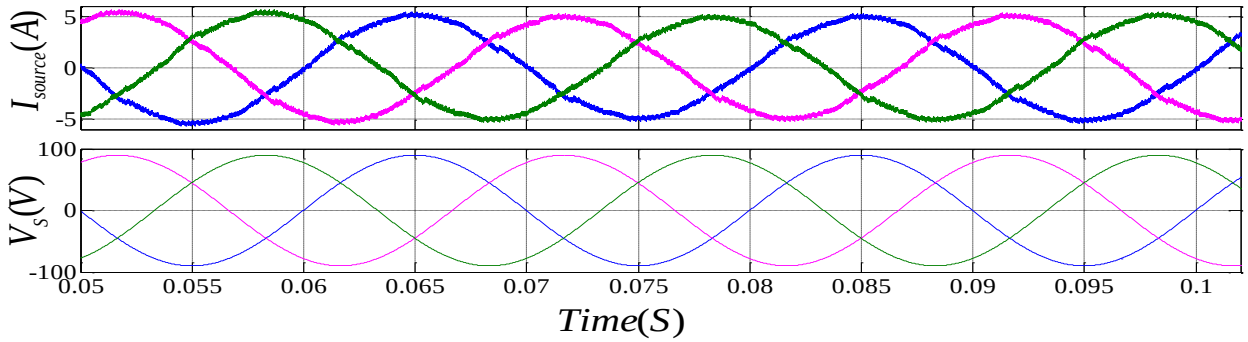

Fig. 5.5. Source voltage (bottom). Source current (top). PFL based controller for three phase APF

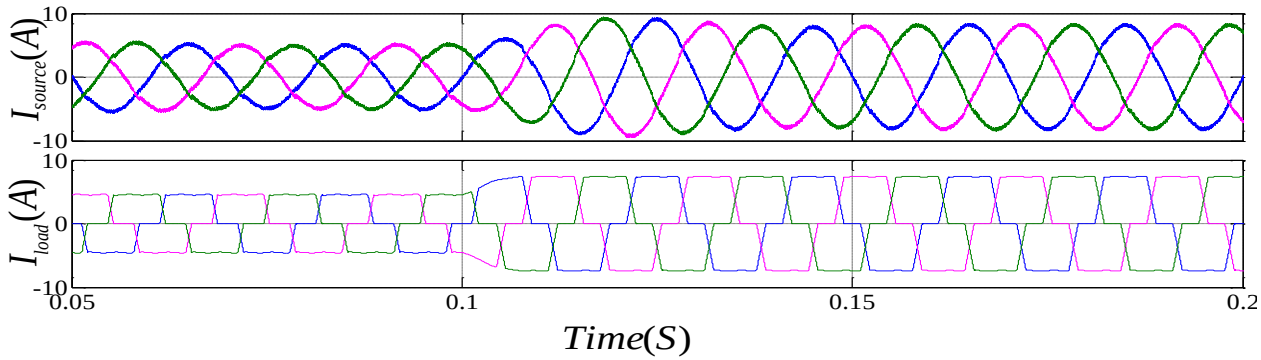

Fig.5.6. Response for load change. Load current (bottom). Source current (top).

PFL based controller for three phase APF

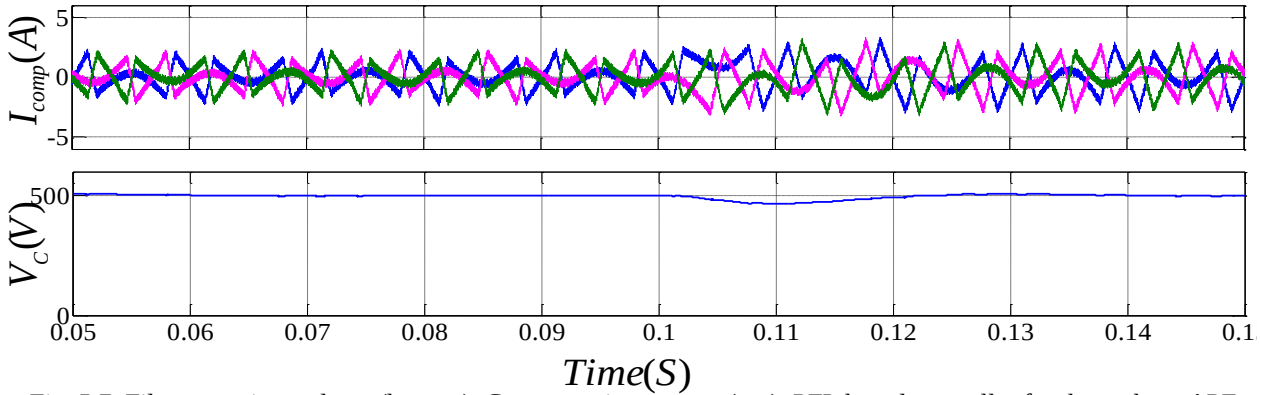

Fig. 5.7. Filter capacitor voltage (bottom). Compensating current (top). PFL based controller for three phase APF

THDs of load current and source voltage are found to be 25.76% and 1% respectively. The waveforms of source voltage and load current for three phase APF are shown in Fig. 5.4. With the PFL based controller source current THD has been reduced to 2.79% (shown in Fig. 5.5). Further, it can be seen that source currents of all three phases are found to be in same phase to that of source voltages of the same phase. To examine the transient response of the proposed controller, simulations are carried out for a sudden load change from peak load current 4A to 8A at 0.1 sec. From Fig. 5.6, it is observed that the settling time of the proposed controller is small. The filter capacitor voltage is maintained approximately at a constant value of 500V in PFL based controller as shown in Fig. 5.7. The inductor current or the compensating current required to compensate the harmonics from source current is also shown in Fig.5.7.

5.6. Chapter summary

In this chapter, a PFL based controller design of three phase shunt APF is reported using its averaged dynamic model. Three phase APF is considered as a MIMO system. Total relative degree of the MIMO system is found by considering the relative degree of each input output pair separately. Stability of internal dynamics of the complete system in PFL based controller is analyzed. Usual pulse width modulation based switching scheme is employed for implementation of the proposed control algorithm in both simulation studies. Finally both MATLAB/Simulink based simulation results are provided to check the performance of the proposed controller. It is found that PFL based controller is a better choice because it provides complete stability of the APF system and reduces the source current THD.

CHAPTER 6

CONCLUSIONS AND SUGGESTIONS FOR FUTURE WORK

6.1. Conclusions

This section reports the overall conclusions of the thesis. In this thesis, three control strategies namely "Analog Sliding Mode Controller", "Fixed Switching Frequency Adaptive Sliding Mode Controller" and "Partial Feedback Linearization based Sliding Mode Controller for single phase shunt APF and one control strategy for three phase shunt APF have been proposed. In all the control strategies, compensating current is controlled using SM control or PFL based control. SM control strategy is applied to APF considering the dynamic model of APF similar to that of model reported in [1]. But PFL based control is applied to shunt APF considering its averaged dynamic model. The averaged dynamic model of both single phase and three phase shunt APF is obtained by averaging coupling inductor current and filter capacitor voltage over a complete switching cycle. Both SM current control strategy and PFL based current control strategy are found robust and easy to implement. But PFL based controller is found more suitable than the SM controller as it improves the performance of APF by analysing the stability of the complete system. It is also observed that reference source current calculation method has an important role in improving the performance of APF. Use of bandpass filter or ANN in the reference source current calculation process makes APF applicable under both nominal source and distorted source. Simulations are carried out to verify the theory in both MATLAB and Multisim platform. Experimental results for PFL based controller has also been carried out and it is found that simulation results agree with experimental results.

6.2. Contributions of the thesis

- An analog sliding mode controller is developed in which a band pass filter is used for reference source current generation. Multisim based simulation is carried out to report the method of analog implementation.

- A fixed switching frequency adaptive sliding mode controller is developed in which combination of ANN and PD controller is used to generate the reference source current and control the filter capacitor voltage.
- Averaged dynamic model of both single phase and three phase systems are derived and using these models, PFL based control technique is applied to both the systems considering their stability.
- Experimental prototype of PFL based controller for single phase APF is built and results are compared with exact feedback linearization of APF via SM control.

6.3. Suggestions for future work

- In ANN weight updating algorithm, a constant value of learning rate is taken. In future step should be taken to vary the learning rate, so that the updating process becomes more fast and accurate.
- All the works have been done considering VSI as APF. In future these works can further be extended to CSI as APF.

REFERENCE

[1] D. A. Torrey and A. M. A. M. Al-Zamel,"Single-phase active power filters for multiple nonlinear loads," *IEEE* Trans. *Power Electron.*, vol. 10, no. 3, pp. 263–272, May 1995.

[2] J. Miret, M. Castilla, J. Matas, J. M. Guerrero, Luis Garcia de Vicuna, "Design of an analog Quasi-steady-state nonlinear current mode controller for single phase active power filter". *IEEE Trans. Ind. Electron.*, vol. 56, no. 12, pp. 4872-4881, Dec 2009.

[3] J. Matas, Luis Garcia de Vicuna, J. Miret, J. M. Guerrero, M. Castilla, "Feedback linearization of single phase active power filter via sliding mode control". *IEEE Trans. power. Electron.*, vol. 23, no. 1, pp. 116-125, Jan 2008.

[4] H. Komurcugil and O. Kukrer, "A new control strategy for single-phase shunt active power filters using a Lyapunov function," *IEEE Trans. Ind. Electron.*, vol. 53, no. 1, pp. 305–312, Feb. 2006.

[5] C.Y.Hsu and H.Y.Wu, "A new single phase active power filter with reduced energy-storage capacity," *IEE proceedings on electric power applications*. vol. 143, no. 1, pp. 25-30, 1996.

[6] M. Angulo, D.A. Ruiz-Caballero, J.Lago, M. L. Heldwein, S.A. Mussa. "Active power filter control strategy with implicit closed-loop current control and resonant controller". *IEEE Trans. Ind. Electron.*, vol.60, no. 7, pp. 2721-2730, july 2013.

[7] P.karuppanan, S.R.Prusty, K.K. Mahapatra, " Adaptive- hysteresis current controller based active power filter for power quality enhancement". *SEISCON*, pp. 1-6, 2011.

[8] P. Salmeron, J.R. Vazquez, "Practical design of a three phase active power line conditioner controlled by artificial neural network". *IEEE Trans. Power delivery,* vol.20, no. 2, pp. 1037-1044, april 2005.

[9] V.B. Sriram, S. SenGupta, A. Patra, "Indirect current control of a single-phase voltage-sourced boost-type bridge converter operated in rectifier mode". *IEEE Trans. power Electron,* vol.18, no.5, pp. 1130-1137, sep 2003.

[10] Siew-Chong Tan, Y.M. Lai, C.K. Tse. , "A unified approach to the design of PWM-base sliding mode controller for basic DC-DC converters in continuous conduction mode". *IEEE Trans. circuits and systems*, vol.53, no.8, pp. 1816-1827, aug 2006.

[11] R.A. DeCarlo, S.H. Zak, G.P. Matthews, "Variable structure control of nonlinear multivariable systems: a tutorial". *Proceedings of IEEE,* vol.76, no.3, pp. 212-232, 1988.

[12] D.O Abdeslam, P Wira, J. Merckle, D Flieller, Y. A Chapuis, "A unified artificial neural network architecture for active power filters". *IEEE Trans. Ind. Electron.*, vol.54, no. 1, pp. 61-76, Feb 2007.

[13] A.Abrishamifar, A.A.Ahamad, M,Mohamadian, "Fixed switching frequency sliding mode control for single-phase unipolar inverter". *IEEE Trans. power Electron*, vol.27, no.5, pp. 2507-2514, may 2012.

[14] F. Pottker, I. Barbi, "Power factor correction of nonlinear loads employing a single phase active power filter: control strategy, design methodology and experimentation". *Power Electron Specialists conference,* vol.1, pp.412-417, 1997.

[15] L. H. Tey, P.L.So and Y. C. Chu, "Improvement of power quality using adaptive shunt active power filter". *IEEE Trans. on power delivery*, vol.20, pp. 1558-1568, 2006.

[16] T. C. Green and J. H. Marks, "Control techniques for active power filters," *Proc. Inst. Elect. Eng.—Elect. Power Appl.* vol. 152, no. 2, pp. 369–381, Mar. 2005.

[17] M. Cirrincione, M. Pucci, and G. Vitale, "A single-phase DG generation unit with shunt active power filter capability by adaptive neural filtering," *IEEE Trans. Ind. Electron.*, vol. 55, no. 5, pp. 2093–2110, May 2008.

[18] H. Akagi, "Trends in active power line conditioners," *IEEE Trans. Power Electron*, vol. 9, no. 3, pp. 263–268, May 1994.

[19] H. Akagi, "Active harmonic filters," *Proc. I EEE* , vol. 93, no. 12, pp. 2128–2141, Dec. 2005

[20] M. El-Habrouk, M. K. Darwish, and P. Mehta, "A survey of active filters and reactive power compensation techniques," in *Proc. I EE Conf. Power Electron. Variable Speed Drives (Conf. Publ. No. 475)*, 2000, pp. 7–12.

[21] M. P. Kazmierkowski and L. Malesani, "Current control techniques for three-phase voltage-source PWM converters: A survey," *IEEE Trans. Ind. Electron.*, vol. 45, no. 5, pp. 691–703, Oct. 1998.

[22] Pottker and I. Barbi, "Power factor correction of non-linear loads employing a single phase active power filter: Control strategy, design methodology and experimentation," in *Proc. IEEE PESC*, St. Louis, MO, Jun. 22–27, 1997, pp. 412–417.

[23] J. C. Wu and H. L. Jou, "Simplified control method for the single-phase active power filter," *Proc. Inst. Elect. Eng.—Elect. Power Appl.*, vol. 143, no. 3, pp. 219–224, May 1996.

[24] G. Escobar, P. R. Martinez, and J. Leyva-Ramos, "Analog circuits to implement repetitive controllers with feed forward for harmonic compensation," *IEEE Trans. Ind. Electron.*, vol. 55, no. 1, pp. 567–573, Feb. 2007.

[25] Haroon I. Yunish and Richard M. Bass, "Comparison of VSI and CSI topologies for single phase active power filter". *IEEE PESC.*, pp.1892-1898, 1996.

[26] N. Gupta and S. P Singh, "Fuzzy logic controlled shunt active power filter for reactive power compensation and harmonic elimination". *ICCCT*, pp. 82-87, 2011.

[27] M. Ranjbar and A shoulaie, "DSP based digital control of single phase shunt active power filter under distorted voltage source". *PEDSTC*, pp.276-281, 2010.

[28] H. L. Jou, J. C. Wu and H. Y. Chu, "New single phase active power filter". *Electric power application, IEEE proc*., vol.141, pp. 129-134, 1994.

[29] Kuo-Kai Shyu, Ming-Ji Yang, Yen-Mo Chen, Yi-Fei Lin, "Model reference adaptive control design for shunt active power filter system". *IEEE Trans. Ind. Electron.*, vol. 55, no. 1, pp. 97–106, 2008.

[30] Chen Fangjing, Chan Zhongren, Wang Hui, Le Jiangyuan, "Research of state exact feedback linearization control of shunt single phase active power filter". *Asia pacific Power and energy engineering conference (APPEEC)*. pp. 1-4, 2010.

[31] Lai Xiaohua, Le Jiangyuan, A novel nonlinear control strategy for single phase APF based on feedback linearization". *International conference on electrical and control engineering(ICECE)*. pp. 3305-3308, 2011.

[32] Zinbo Liu, Wenlong ming, Fanghong gao, " A new control strategy for improving performance of boost DC/DC converter based on input-output feedback linearization". *8th world congress on intelligent control and automotion (WCICA)* pp. 2439-2444, 2010.

[33] Huijun Zheng, Dingxin Shuai, "Nonlinear control of boost converter by state feedback exact linearization". *24th chinese Control and decision conference (CCDC)* pp. 3502-3506, 2012.

[34] S.S. Sastry, A Isidori, "Adaptive control of linearizable systems" *IEEE Trans. On automatic control.*, vol. 34, no. 11, pp. 1123--1131, Dec 1989.

[35] Dong-Eok Kim, Dong-Choon Lee, "Feedback linearization control of three phase UPS inverter system". *IEEE Trans. Ind. Electron.*, vol. 57, no. 3, pp. 963-968, 2009.

[36] M. Routimo, M. Salo, H. Tuusa, "Comparison of voltage-source and current-source shunt active power filters" *IEEE Trans. Power Electron.*, vol. 22, no. 2, pp. 636–643, 2007.

[37] L. Benchaita, S. Saadata, A. Salem nia, " A comparison of voltage source and current source shunt active filter by simulation and experimentation" *IEEE Trans. Power Systems.*, vol. 14, no. 2, pp. 642–647, 1999.

[38] R. Devaraj, S. Saetieo,D. A. Torrey, " The design and implementation of a three phase active power filter based on sliding mode control" *IEEE Trans. Industry Application*, vol. 31, no. 5, pp. 993–1000, 1995.

[39] A. Chaoui, J-P. Gaubert, F. Krim, L. Rambault, " On the design of shunt active filter for improving power quality" *IEEE International Symposium on Industrial Electronics*, pp. 31–37, 2008.

[40] A. Bhattacharya and C. Chakraborty, " A shunt active power filter with enhanced performance using ANN-based predictive and adaptive controllers" *IEEE Trans. Power Electron.*, vol. 58, no. 2, pp. 421–428, 2011.

[41] M. Marimelli and A. D. Aquila, "Improved current control of active power filter using genetic algorithms" *IEEE Symposium on Industrial Electronics*, pp. 98–103, 2004.

[42] S. Saad and L. Zellouma " Fuzzy logic controller for three phase shunt active power filter compensating harmonics and reactive power" *Electric Power System Research*, vol. 79, no.10, pp. 1337–1341, 2009.

[43] R. Belaidi, A. Haddouche, H. Guendouz, "Fuzzy logic controller based three phase shunt active power filter for compensating harmonics and reactive power under unbalanced mains voltage" " *Energy Procedia*, no.18, pp. 560–570, 2012.

[44] Karuppanan P, K.K. Mahapatra, "PI and fuzzy logic controllers for shunt active power filter-A report" " *ISA Trans.*, vol. 51, no.1, pp. 1337–1341, 2009.

[45] P. Kumar and A. Mahajan, "Soft computing techniques for the control of active power filter" *IEEE Trans. Power Delivery.*, vol. 24, no. 1, pp. 452–461, 2009.

[46] L. Saribulut, A. Teke, M. Tumay, "Artificial neural network based discrete fuzzy logic controlled active power filter" *IET Power Electronics.*, vol. 7, no. 6, pp. 1536–1546, 2014.

[47] M. EI-Habrouk and M. K. Darwish, "A new control technique for active power filters using combined genetic algorithm/ conventional analysis" *IEEE Trans. Ind. Electron.,* vol. 49, no. 1, pp. 58–66, 2002.

[48] J. Dixon, J. Contardo, L. Moran, "DC link fuzzy control for an active power filter, sensing the line current only" *in Proc. IEEE Power Eng. Soc. Com*. pp. 1109–1113, 1997.

[49] H. Akagi, Y. Kanazaya, and A. Nabae, " Instantaneous reactive power compensators compromising switching devices without energy storage component" *IEEE Trans. Industry Application*, vol. 20, no. 3, pp. 625–630, 1984.

[50] S. Bhattacharaya, D. M. Divan, B. Banarji, "Synchronous reference frame harmonic isolator using series active filter", *Proc. 4th EPE, Florence*, vol. 3, pp. 030–035, 1991.

[51] E. H.Watanable, R. M. Stephan, M. Aredes, "New concept of active and reactive power in electric systems with genetic loads", *IEEE Trans. Power Delivery.*, vol. 8, no. 2, pp. 697–703, 1993.

[52] S. Reyes, P. Salmeron, H. Kim, "Instantaneous reactive power theory applied to active power filter compensation: different approaches, assessment and experimental results" *IEEE Trans. Ind. Electron.,* vol. 55, no. 1, pp. 184–196, 2008.

[53] M. Kale, E. Ozdemir, " An adaptive hysteresis band current controller for shunt active power filter" *Electric Power System Research,* vol. 73, no.2, pp. 113–119, 2005.

[54] G. H. Bode, D. G. Holmes, "Implementation of three level hysteresis current control for single phase voltage source inverter", *Power Electron. Specialists conference,* vol.1, pp.33-38, 2000.

[55] B. Mazari, F. Mekri, "Fuzzy hysteresis control and parameter optimization of shunt active power filter" *Journal of Information Science and Engineering,* vol.21, pp.1139-1156, 2005.

[56] S. Oucheriah, L. Guo, " PWM based adaptive sliding mode control for boost DC-DC converters", *IEEE Trans. Ind. Electron.,* vol. 60, no. 8, pp. 3291–3300, 2013.

[57] E. Bianconi, J. Calvente, R. Giral, E. Mamarelis, G. Petrone, C. A. Ramos-Paja, M.Vitelli, " A fast current based MPPT technique employing sliding mode control", *IEEE Trans. Ind. Electron.,* vol. 60, no. 3, pp. 1168-1178, 2013.

[58] F. Betin, D. Pinchon, Gerard-Andre Capolino, "A time-varying sliding surface for robust position control of a DC motor drive", *IEEE Trans. Ind. Electron.*, vol. 49, no. 2, pp. 462–472, 2002.

[59] M. A. Mahmud, H. R. Pota, M. J. Hossain, "Dynamic stability of three phase grid connected photovoltaic system using zero dynamic design approach", *IEEE Journal of Photovoltaics.*, vol. 2, no. 4, pp. 564–571, 2012.

[60] M. A. Mahmud, H. R. Pota, M. J. Hossain, N. K. Roy, " Robust partial feedback linearizing stabilization scheme for three phase grid connected photo voltaic system", *IEEE Journal of Photovoltaics.*, vol. 4, no. 1, pp. 423–431, 2014.

[61] Jean-Jacques E. Slotine, Weiping Li, *Applied Nonlinear Control*. New Jersey: Prentice Hall, 1991.

Thesis Dissemination

1. S.R. Mohapatra and P.K. Ray "A Fixed Switching Frequency Adaptive Sliding Mode Controller for Shunt Active Power Filter System", *IEEE Conference Tencon-2014*, Bangkok, Thailand, 22-25 October, 2014
2. S.R. Mohapatra and P.K. Ray "Design of an Analog Sliding Mode Controller for Single Phase Active Power Filter", *Recent Advances in Power, Energy and Control (RAPEC-2013*), 22-24 November 2013, NIT Rourkela
3. S.R. Mohapatra, P.K. Ray and B. Subudhi "A Partial Feedback Linearization based Approach to Shunt Active Power Filter Design", *IEEE Transactions on circuits and systems* (Submitted in Dec-2014)
4. S.R. Mohapatra and P.K. Ray "Partial Feedback Linearization of Three Phase Shunt Active Power Filter", *ISA Transactions (Elsevier)* (Submitted in Dec-2014)
5. S.R. Mohapatra and P.K. Ray "A Constant switching Frequency adaptive Sliding Mode Current Control Design and Simulation for Shunt Active Power Filter System ", *Journal of Mathematics and Computers in Simulation* (*Elsevier*) , (Submitted in Apr -2014, Under Review)

Soumya Ranjan Mohapatra

He born to Smt. Chunibala Mohapatra and Mr. Niranjan Mohapatra in 27th May, 1989 in Nimapara, Puri, Odisha.

Email: soumyaranjan597@gmail.com

Phone: +919040504991

Academic Profile:

S.No	Degree/	Board/University	Percentage/ CGPA
1	M.Tech (Res) (continuing)	National Institute of Technology Rourkela, India	9.44 (CGPA upto 4th sem)
2	B.Tech (Electronics & Instrumentation Engineering)	Dr. M.G.R University, Chennai	8.21 (CGPA)
3	12th	Council of Higher Secondary Education, Odisha	77.7%
4	10th	Board of Secondary Education, Odisha	86.1%

Publications:

He has published two conference papers and communicated three journal papers.

Present Address:

At-seulasahi, Po-chanarapada, Via-Nimapara, Dist-puri, Odisha, Pin-752106

,